Nsp1 of SARS-CoV-2 Stimulates Host Translation Termination

Alexey Shuvalov[1], Ekaterina Shuvalova[2], Nikita Biziaev[2], Elizaveta Sokolova[1], Konstantin Evmenov[2], Tatyana Egorova[1] and Elena Alkalaeva[1,*]

[1] Center for Precision Genome Editing and Genetic Technologies for Biomedicine, Engelhardt Institute of Molecular Biology, Russian Academy of Sciences, 119991 Moscow, Russia

[2] Engelhardt Institute of Molecular Biology, Russian Academy of Sciences, 119991 Moscow, Russia

*Correspondence: Tel: +74991359977; Fax: +74991351405; Email: alkalaeva@eimb.ru

SUMMARY

The Nsp1 protein of SARS-CoV-2 regulates the translation of host and viral mRNAs in cells. Nsp1 inhibits host translation initiation by binding to the entry channel of the 40S ribosome subunit. The structural study of SARS-CoV-2 Nsp1-ribosomal complexes reported post-termination 80S complex containing Nsp1 and the eRF1 and ABCE1 proteins. Considering the presence of Nsp1 in the post-termination 80S ribosomal complex simultaneously with eRF1, we hypothesized that Nsp1 may be involved in translation termination. We show the direct influence of Nsp1 on translation termination. Using a cell-free translation system and reconstituted *in vitro* translation system, we reveal that Nsp1 stimulates translation termination in the stop codon recognition stage. We identify that activity of Nsp1 in translation termination is localized in its N-terminal domain. The data obtained will enable an investigation of new classes of potential therapeutic agents from coronavirus infection competing with Nsp1 for binding with the termination complex.

INTRODUCTION

Currently, the new coronavirus infection COVID-19 pandemic continues around the world, having already killed more than 1 million people. The causative agent of COVID-19 is Severe Acute Respiratory Syndrome Coronavirus 2 (SARS-CoV-2), which belongs to the beta-coronavirus group (Zhu et al., 2020). Its genome consists of a single-stranded (+) RNA, approximately 30,000 nt long, containing 14 open reading frames (ORFs) encoding an amino acid sequence of 27 proteins. The two overlapping 5'-end frames ORF1a and ORF1b encode large polypeptides (490 and 794 kDa), which are subsequently proteolytically cleaved by viral proteases (Nsp3 and Nsp5), generating the unstructured proteins Nsp1-Nsp16. The ORF1b polypeptide arises during a -1 frameshift just before the ORF1a stop codon. The RNA-dependent RNA polymerase NSP12 generated during the cleavage of ORF1b ensures the replication of the viral genome, also producing additional truncated RNA products with open reading frames for the synthesis of the remaining SARS-CoV-2 proteins (Kim et al., 2020b; Wu et al., 2020; Zhou et al., 2020). It has been shown that among all SARS-CoV-2 proteins, Nsp1 is a major viral factor that affects cellular viability (Yuan et al., 2020).

Nsp1 is the first protein produced by a virus. It affects the vital activity of the infected cell and is necessary for the development of viral particles. Nsp1 is overexpressed in infected cells, induces apoptosis, and alters the transcriptional profile of cells, in particular, blocking the transcription of genes responsible for cell metabolism, regulation of the cell cycle, mitochondrial function, antigen presentation, ubiquitin/proteasome pathways, and protein synthesis (Yuan et al., 2020). Moreover, Nsp1 also directly inhibits translation both *in vitro* in the cell-free translation systems and *in vivo* in the cells (Banerjee et al., 2020; Schubert et al., 2020; Shi et al., 2020; Tidu et al., 2020; Yuan et al., 2020). Therewith, viral mRNAs are less susceptible to translation inhibition due to the presence of an SL1 hairpin in their 5'UTR (Banerjee et al., 2020; Schubert et al., 2020; Shi et al., 2020; Tidu et al., 2020). Nsp1-mediated inhibition of translation leads to suppression of the host interferon response, which is one of the main mechanisms of cellular defense against viral replication (Banerjee et al., 2020; Thoms et al., 2020; Xia et al., 2020).

Nsp1 of the SARS-CoV-2 virus is a small protein of 180 amino acid residues, consisting of N- and C-terminal domains connected by an unstructured linker (Shi et al., 2020; Wu et al., 2020). The N-domain of this protein interacts with the 5 'UTR of SARS-CoV-2 mRNA, which is necessary for its efficient translation (Shi et al., 2020). Mutations in the N-domain also lead to a decrease in the level of apoptosis of infected cells (Yuan et al., 2020). The C-domain of Nsp1 binds to the entry channel of the 40S ribosome subunit. In this case, the 40S subunit associated with Nsp1 binds to mRNA much worse and is unable to form a native translation initiation complex. Thus, Nsp1 inhibits the initiation of host mRNA translation (Banerjee et al., 2020; Lapointe et al.,

2020; Schubert et al., 2020; Shi et al., 2020; Thoms et al., 2020; Tidu et al., 2020; Yuan et al., 2020). In addition to free 40S subunits, Nsp1 SARS-CoV2 is also found in aberrant 48S initiator complexes and 80S ribosomes (Lapointe et al., 2020; Schubert et al., 2020; Thoms et al., 2020; Yuan et al., 2020). It should be noted that binding to the 40S subunit of homologous Nsp1 in closely related SARS-CoV also does not block the formation of the 48S initiator complex but inhibits the attachment of the 60S subunit to it and causes inhibition of the translation initiation (Kamitani et al., 2009). We noticed that some of the resolved 80S ribosomes with Nsp1 SARS-CoV2 also contain proteins involved in translation termination and ribosome recycling: the eukaryotic release factor eRF1 and ABCE1 (Thoms et al., 2020). This led us to think about the possible role of Nsp1 in translation termination.

Translation termination is the final stage of protein biosynthesis, in which the nascent polypeptide releases from the ribosome. Translation termination begins when one of the three stop codons appears in the A site of the ribosome (Jackson et al., 2012). The eukaryotic ribosome binds to eRF1, recognizing all three stop codons (Brown et al., 2015; Frolova et al., 1994; Kryuchkova et al., 2013; Matheisl et al., 2015; Song et al., 2000) . A partner protein of eRF1 is eRF3, a GTPase activating eRF1 (Alkalaeva et al., 2006; Cheng et al., 2009; Frolova et al., 1996; Shao et al., 2016; Taylor et al., 2012). Binding of the eRF1-eRF3-GTP complex with the stop codon stimulates GTPase activity of eRF3, which, in turn, causes a conformational change of eRF1 (Cheng et al., 2009). As a result, the catalytic GGQ motif of eRF1 is positioned at the peptidyl transferase center of the ribosome. This induces the hydrolysis of peptidyl-tRNA and the release of the synthesized protein (Alkalaeva et al., 2006; Brown et al., 2015; Frolova et al., 1999; Jackson et al., 2012; Matheisl et al., 2015; Song et al., 2000). Termination of translation is one of the critical stages of protein biosynthesis because its suppression allows for inhibiting both the release of peptides from the ribosomes and the transition of the ribosomes to recycling, consequently, to prevent a new round of translation.

The simultaneous localization of eRF1 and Nsp1 of SARS-CoV-2 in the 80S ribosomes, revealed by structural study (Thoms et al., 2020), indicates a possible role of Nsp1 in translation termination, which has not previously been observed. To study the effect of Nsp1 on the termination of host translation, we used a reconstituted mammalian translation system (Alkalaeva et al., 2006) as well as pre-termination complexes (preTCs) purified from rabbit reticulocyte lysate (RRL) (Susorov et al., 2020). We demonstrated that Nsp1 of SARS-CoV-2 stimulates translation termination and determines the stage of termination at which it works. Direct involvement in translation termination of Nsp1 was confirmed by studying activities of the domains and mutants of Nsp1. The data obtained allow us to propose a possible mechanism of control of translation on the stage of termination by SARS-CoV-2 Nsp1.

RESULTS

Nsp1 stimulates peptide release

To study the activity of Nsp1 in translation termination, the codon-optimized Nsp1 sequence encoding SARS-CoV-2 Nsp1 was cloned into the petSUMO vector and expressed in *E. coli* BL21 cells. The resulting wild-type Nsp1 without any tag was used in the experiments. We first verified the ability of the recombinant Nsp1 to inhibit translation. For this purpose, translation of Nluc mRNA in RRL was detected in the presence of Nsp1 (Fig. 1A). We confirmed that our preparation of the recombinant Nsp1 without any tags significantly inhibited the translation of Nluc mRNA in the cell-free system.

The obtained protein was used to study the effect of SARS-CoV-2 Nsp1 on translation termination. The result of translation termination is the hydrolysis of peptidyl-tRNA and the release of the nascent peptide from the ribosome. We performed an analysis of a peptide release efficiency using a Termi-Luc approach developed recently by Susorov et al. (2020). PreTCs, containing NanoLuc luciferase (Nluc) located at the P site of the ribosome in the peptidyl-tRNA form, were purified from the RRL. The addition of the release factors to the purified pretermination complex (preTC) triggers peptidyl-tRNA hydrolysis and induces the release of Nluc from the ribosome. Human release factors eRF1 and eRF3a, together with Nsp1, were added to the preTC, and the luminescence was measured as a function of time. The data obtained showed that Nsp1 significantly stimulates translation termination induced by eRF1 alone and by the complex of eRF1-eRF3a (Fig. 1B). As a negative control we used eukaryotic initiation translation factor eIF1A, which is of a similar size and binds close to the Nsp1 binding site on the ribosome. Therefore, the presence of Nsp1, together with eRF1 in the 80S ribosomal complexes obtained earlier (Thoms et al., 2020), reflects its functional significance in translation termination.

Nsp1 stimulates the termination complexes formation

To study a molecular mechanism of the stimulation of translation termination by Nsp1, we tested its activity on the purified preTCs obtained in the reconstituted translation system (Alkalaeva et al., 2006). We assembled preTCs from individual components on the model MVHL mRNAs with the UAA stop codon and purified them by centrifugation in a sucrose density gradient. These complexes were then used to test the effect of Nsp1 on the formation of termination complexes (TCs) by fluorescent toe-print analysis, which allows for detecting the position of ribosomal complexes on mRNA. When stop codon is recognized by eRF1, the ribosome “pulls” into the A site an additional nucleotide from the 3'-region of the mRNA, which is detected in toe-print analysis as a single or double nucleotide shift of the ribosomal complex (Alkalaeva et al., 2006; Egorova et al., 2019).

Toe-print analysis showed that the addition of Nsp1 to the preTC with the release factor eRF1 increases the amount of formed TC (Fig. 2A). As a negative control, we also used eIF1A. In the presence of both release factors (eRF1 and eRF3a) and GTP, Nsp1 stimulates the formation of the TC (Fig. 2B).

To determine the stage of termination during which Nsp1 activates TC formation, we tested the activity of the eRF1(AGQ) mutant, which is unable to induce hydrolysis of peptidyl-tRNA. We observed that Nsp1 stimulates TC formation by eRF1(AGQ) even stronger than by the wild-type eRF1 (Fig. 2A). Likewise, in the presence of the eRF1(AGQ)-eRF3a complex, we observed significant stimulation of TC formation by Nsp1 (Fig. 2B). Thus, we concluded that Nsp1 stimulates translation termination before peptide release either during the binding of eRF1 with the stop codon or during GTP hydrolysis catalyzed by eRF3a.

Nsp1 does not influence the GTPase activity of eRF3a

One of the critical stages of translation termination is the GTP hydrolysis performed by eRF3, which occurs after the eRF1-eRF3 binding to the stop codon in the ribosome. This is followed by a conformational change of the TC and positioning of eRF1 in the peptidyl-transferase center of the ribosome (Cheng et al., 2009). By analyzing the GTPase activity of eRF3a in the presence of eRF1, 80S ribosome, and Nsp1, we demonstrated no effect of Nsp1 on the hydrolysis of GTP (Fig. 3A). We confirmed this finding by analyzing the efficiency of TC formation in the presence of a non-hydrolysable GTP analogue, GDPCP, using toe-printing assay. The addition of the GDPCP to eRF1 and eRF3a did not prevent stimulation of TC formation by Nsp1 similar to that observed in the presence of GTP (Fig. 3B). Therefore, Nsp1 stimulation activity in translation termination appears before GTP hydrolysis catalyzed by eRF3.

Additionally, we tested the ability of Nsp1 to stimulate peptide release induced by truncation from the C-end form of eRF1, NM-eRF1, which is unable to interact with eRF3a. We observed the same level of peptide release stimulation by Nsp1, as in the case of full-length eRF1 (Fig. 3C). The minimal required part of the release factor to be activated by Nsp1 is its stop codon recognition domain. This once again confirms our conclusion that the GTPase activity of eRF3 on the ribosome does not depend on Nsp1, and the stimulation of translation termination by Nsp1 occurs on the stage of stop codon recognition.

Effects of mutations of Nsp1 on its activity in translation termination

To find critical regions of Nsp1 to perform its function during termination, we obtained five mutant forms of Nsp1: K164A/H165A (KH/AA), Y154A/F157A (YF/AA), R171E/R175E (RR/EE), R124S/K125E (RK/SE), and N128S/K129E (NK/SE), and we truncated for 12 amino acids from the N-terminus form of Nsp1 (ΔNsp1), described previously as proteins that lost activity in translation or are important for cell apoptosis (Fig. 4A) (Schubert et al., 2020; Thoms et al., 2020;

Yuan et al., 2020). The mutant proteins KH/AA, YF/AA, and RR/EE were unable to suppress translation in the cell-free system (Fig. 4B), similarly to previous studies (Schubert et al., 2020; Thoms et al., 2020). However, the mutants RK/SE, NK/SE, and ΔNsp1 decreased the translation of the Nluc in cell-free system similarly to the wild-type Nsp1 (Fig. 4B). On the other hand, the mutants KH/AA and YF/AA stimulated peptide release in the presence of eRF1 alone and the eRF1-eRF3a complex similarly to Nsp1 (Fig. 4C). However, the mutants RR/EE, RK/SE, NK/SE, and ΔNsp1 lost the ability to stimulate peptide release (Fig. 4C).

TC formation analysis of the same mutants showed that the proteins KH/AA and YF/AA demonstrated the same activity as Nsp1 wt (Fig. S1). On the contrary, the mutants RR/EE, RK/SE, NK/SE, and ΔNsp1 did not stimulate the formation of TC (Fig. S1). Therefore, TC formation analysis confirmed the results obtained by the peptide release assay.

Summarizing the obtained results, we can conclude that different parts of Nsp1 are responsible for different activities of this protein in translation. Analysis of mutant activities indicated that the C domain of Nsp1 is involved in translation repression via binding with the 40S subunit, which was shown by structural analysis (Schubert et al., 2020; Thoms et al., 2020; Yuan et al., 2020), but the N domain of Nsp1 is responsible for its activation in translation termination.

We also tested 3xFLAG-tagged Nsp1 (3xFLAG-Nsp1) in peptide release and TC formation analysis, as this form of Nsp1 has been used in different structural and biochemical studies (Schubert et al., 2020; Thoms et al., 2020; Yuan et al., 2020). Interestingly, 3xFLAG-Nsp1 did not suppress translation of Nluc mRNA in the cell-free system (Fig. S2A). However, both in the presence of eRF1 and in the presence of the eRF1-eRF3a-GTP complex, 3xFLAG-Nsp1 stimulated TC formation and peptidyl-tRNA hydrolysis, like wild-type Nsp1 (Fig. S2B,C). Thus, 3xFLAG does not interfere with the functioning of Nsp1 in translation termination but prevents suppression of protein translation in the cell-free system.

N and C domains of Nsp1 lose their function in translation inhibition and termination activation

To confirm the suggestion that domains of Nsp1 have different functions in the translation, we tested the effect of the individual Nsp1 domains on the cell-free translation and peptide release. We constructed N and C domains of Nsp1 by splitting the linker sequence in the middle. As a result, the N domain contained 1-138 amino acid residues, and the C domain contained 139-180 amino acid residues (Fig. 4A). Unfortunately, both domains lost their function in suppressing NLuc cell-free translation (Fig. 5A) and did not stimulate hydrolysis of peptidyl-tRNA in the presence of eRF1 or the eRF1-eRF3a complex (Fig. 5B). Only the N domain of Nsp1 slightly improved the peptide release in the presence of eRF1 with eRF3a (Fig 5B).

Activities of the N and the C domains of Nsp1 were also checked by TC formation analysis. We observed the activity of domains like in the peptide release. The C domain of Nsp1 was unable to stimulate TC formation, and the N domain slightly stimulated TC formation in the presence of eRF1 (Fig.5C). Thus, we have shown that the functioning of Nsp1, both in the translation termination and cell-free translation, requires the presence of the full-length protein.

Nsp1 affects premature stop codon readthrough in the RRL

After testing the effect of Nsp1 on termination in pure systems, it was interesting to observe the effect of Nsp1 on a readthrough of the premature termination codon (PTC) in the lysate containing the full translational apparatus. For this, we designed three pairs of NLuc mRNA to reveal the PTC readthrough level. The mRNA constructions included β-globin 5'UTR, the coding sequence of the first 13 amino acids of human β-globin with or without different PTC, followed by the three different weak 3'-contexts, NLuc CDS, and 3'UTR with 50 nt poly(A) (Fig. 6A). The weak contexts were used in order to increase basic level of the readthrough, which allowed us to detect even a weak effect on translation termination.

We determined that Nsp1 increased the readthrough on UGA and UAG PTCs, followed by the weak contexts, weak and dystrophin, respectively. The readthrough level in the presence of Nsp1 was about 11% for UGA, in comparison to 9% in the absence of Nsp1, and about 3% for UAG in the presence of Nsp1, in comparison to 2,5% in the absence of Nsp1 (Fig. 6B). Almost complete suppression of translation was detected in the presence of Nsp1 for NLuc-UAA mRNA, although the readthrough without Nsp1 for this mRNA was around 1.25% (Fig. 6B). So the readthrough level for the UAA stop codon could not be detected. Thus, we observed that Nsp1 increases the readthrough efficiency in the PTC model for UAG and UGA codons. The PTC readthrough results contradict the previous data, because increasing readthrough efficiency means decreasing termination of translation. To understand what Nsp1 activity leads to this result, we determined PTC readthrough efficiency for the KH/AA mutant of Nsp1 (Fig. 6B). As we shown the KH/AA mutant lacks translation suppression activity and keeps stimulating termination activity (Fig. 4B,C). In the presence of the KH/AA protein the PTC readthrough was similar to detected in the control experiments performed in the absence of Nsp1. Therefore, the effect of Nsp1 on the PTC readthrough is controlled by the binding of its C domain with the 40S.

In order to understand how Nsp1 affects translation termination at these stop codons *in vitro*, we studied the efficiency of TC formation on the model mRNAs with the same stop codons. We revealed that in all three stop codons, Nsp1 significantly stimulated TC formation in the presence of the eRF1-eRF3-GTP complex (Fig. 6C). That confirms an independence of the PTC readthrough level from the Nsp1 activity in translation termination.

Gentamicin and mefloquine influence on Nsp1-mediated termination stimulation

To further study the mechanism of Nsp1 activation of translation termination, we tested two types of therapeutic agents affecting different parts of termination complex—aminoglycoside antibiotic gentamicin and antimalaria agent mefloquine. PTC readthrough stimulation and binding with the different parts of the 80S ribosome, especially with the ribosomal decoding center, were shown for gentamicin (Bidou et al., 2004; Prokhorova et al., 2017; Wilhelm et al., 1978). Binding to the ribosome GTPase-associated center of the *Plasmodium falciparum* 80S ribosome (Wong et al., 2017) and PTC readthrough promotion in the presence of G418 (Ferguson et al., 2019) were shown for mefloquine. Furthermore, debate on the possible use of mefloquine in the treatment of COVID19 did not stop.

Since Nsp1 activates translation termination, it can be assumed that these antibiotics can compete with Nsp1, influencing termination activity. Thus, we tested the effect of gentamicin and mefloquine on Nsp1-mediated termination stimulation in peptide release and TC formation assays. In the peptide release reaction, neither antibiotic (concentration of 100 μM) had any effect in the presence of eRF1 and eRF3a together; however, in the presence of Nsp1, gentamicin stimulated peptide release. In contrast, in the presence of Nsp1, mefloquine decreased peptidyl-tRNA hydrolysis (Fig. 7A). In the presence of eRF1 alone, gentamicin inhibited peptide hydrolysis, whereas mefloquine did not affect it. When Nsp1 was added to peptide release reaction with eRF1, mefloquine stimulated the peptide release, while gentamicin non-significantly suppressed the Nsp1 effect on termination (Fig. 7A).

The TC formation assay in the presence of eRF1 alone confirms the results of the peptide release (Fig. 7A). In all cases, mefloquine stimulates TC formation, and gentamicin suppresses it, independently of the presence of Nsp1. However, in the presence of both release factors eRF1 and eRF3, we detected only the inhibition of TC formation in the absence of Nsp1, and in all other cases, neither gentamicin nor mefloquine affect TC formation. It may be bound with the lower stability of the TC in the presence of eRF3a, and we were unable to determine the increased TC formation in those cases. To test this hypothesis we determined the influence of antibiotics on TC formation efficiency in the presence of eRF1-eRF3 and GDPCD. As GDPCD is unable to be hydrolyzed be eRF3, such TC stay in the intermediate state and unable to dissociate from the ribosome. In this case we observed more pronounced activation of TC formation by mefloquine and gentamicin in the presence of Nsp1 which support our suggestion of partial TC dissociation after peptide release. However, in the presence of mefloquine and Nsp1 we detected increased amount of the TC (Fig. 7B) which contradicts with the peptide release result (Fig. 7A). Probably the suppression of Nsp1 by mefloquine somehow depends on the GTP hydrolysis performed by eRF3, so in the presence of GDPCP this activity is unobtainable.

Summarizing the obtained results, we conclude that analyzed antibiotics differently influence peptide release in the presence of Nsp1, which points out the difficult mechanism of the action of the Nsp1 in translation termination.

DISCUSSION

The role of Nsp1 in the novel coronavirus SARS-CoV-2 in the initiation of host translation has previously been reported (Banerjee et al., 2020; Lapointe et al., 2020; Schubert et al., 2020; Shi et al., 2020; Thoms et al., 2020; Tidu et al., 2020; Yuan et al., 2020). Additionally, it was shown that Nsp1 is localized in the 80S ribosome simultaneously with eRF1 and ABCE1 (Thoms et al., 2020) . In the present study, we demonstrate the role of Nsp1 in translation termination. We show the activity of Nsp1 at different stages of termination (Fig. 1–3) and identify the regions of Nsp1 important for its functioning in translation termination (Fig. 4). Overall, we propose that Nsp1 stimulates translation termination in the step of stop codon recognition by its N-terminal domain.

At the same time, Nsp1 suppresses cell translation at the initiation stage via binding to the 40S ribosome subunit to transfer components of protein biosynthesis into the translation of virus proteins (Banerjee et al., 2020; Lapointe et al., 2020; Schubert et al., 2020; Shi et al., 2020; Thoms et al., 2020; Tidu et al., 2020; Yuan et al., 2020). However, the entire process of translation cannot be stopped by only suppressing initiation because those mRNAs that have already passed the initiation stage continue to be translated at the stages of elongation and termination. To disrupt the translation of such mRNAs, it would be reasonable to stimulate termination at the stop codons and remove the release factors and 40S ribosome subunits from the pool of active components. We assume that Nsp1 is involved in this process. By stimulating termination in translating mRNA, it binds to the 40S ribosome subunits and can prevent host initiation of translation. It should be noted that SARS-CoV-2 mRNA contains two long ORFs for the translation of 16 proteins. They contain only two stop codons, so the elimination of the 40S subunits by NSP1 after translation termination preferentially involves ribosomes that translate host mRNAs and do affect the translation of the viral proteins encoded in the first two ORFs.

As we have shown that Nsp1 can take part in translation termination by stimulating its first stage, stop codon recognition, antibiotics that induce PTC readthrough may be potentially useful in fighting the COVID infection. We tested in translation termination of two types of readthrough-inducing agents—the aminoglycoside antibiotic gentamicin and the antimalarial drug mefloquine (Bidou et al., 2004; Ferguson et al., 2019). We observed opposite effects of these substances at Nsp1-dependent stimulation of translation termination. Gentamicin stimulated the termination of translation performed by the pair of release factors eRF1 and eRF3a, while at the same time, mefloquine decreased it. This can be explained by the fact that gentamicin and mefloquine interact with the different regions of the 80S ribosome (Prokhorova et al., 2017; Wong et al., 2017), and consequently, they affect different steps of translation termination. Taking the data on the possible

use of mefloquine as an antiviral agent for COVID treatment into account, we think that inhibition of Nsp1 functioning during termination by this drug could be a possible mechanism of its suppression of the SARS-CoV-2 infection. We assume that mefloquine could bind with the GTPase center of the human 80S ribosome by analogy with *Plasmodium falciparum* 80S (Wong et al., 2017) and displace eRF3 from the ribosome or somehow influence its activity in translation. This assumption should definitely be tested in the future, and of course, the possible influence of gentamicin and other aminoglycoside antibiotics on the SARS-CoV-2 infection should not be ignored either.

MATERIAL AND METHODS RESOURCE AVAILABILITY

Lead Contact

Further information and requests for resources and reagents should be directed to and will be fulfilled by the Lead Contact, Elena Alkalaeva (alkalaeva@eimb.ru).

Materials Availability

Plasmids generated in this study are planned to be deposited to Addgene.

Data and Code Availability

This study did not generate or analyze any datasets and code.

EXPERIMENTAL MODEL AND SUBJECT DETAILS

To *in vitro* translation and Termi-Luc peptide release assays, Rabbit Reticulocyte Lysate (RRL) (Green Hectares, USA) was used.

To purify native proteins, RRL (Green Hectares, USA) or HeLa (Ipracell, Belgium) lysates were used.

METHOD DETAILS

Nsp1 cloning and purification

Codon-optimized Nsp1 wt was amplified by PCR with Q5 polymerase (NEB) from the plasmid pDONR207 SARS-CoV-2 NSP1, which was a gift from Fritz Roth (Addgene plasmid # 141255; http://n2t.net/addgene:141255; RRID:Addgene_141255) (Kim et al., 2020a) using primers NSP1_F, NSP1_R. petSUMO (Invitrogen) vector was amplified by PCR with Q5 polymerase (NEB) using primers petSUMO_F, petSUMO_R. The petSUMO_Nsp1_WT construct was obtained using PCR-products with Gibson Assembly® Master Mix (NEB), according to manufacturer's protocol. N (1-137 aa) and C (139-180 aa) Nsp1 domains were cloned into petSUMO using primers NSP1_N_R and NSP1_C_F, as well as ΔNsp1 with the primer ΔNSP1_F. Nsp1 mutants RK/SE, NK/SE, KH/AA, YF/AA, RR/EE were made with use of QuikChange Site-Directed Mutagenesis Kit (Agilent), according to manufacturer's protocol. 3xFLAG was amplified by PCR with Q5 polymerase (NEB) from our construct using primers 3xFLAG_F and 3xFLAG_R and cloned into petSUMO_NSP1_WT vector using Gibson Assembly® Master Mix (NEB). The resulting proteins were expressed in *Escherichia coli* BL21(DE3) cells (Invitrogen) after induction by 0.5 mM isopropyl β-D-1-thiogalactopyranoside at 18°C overnight, followed by purification using a Ni-NTA gravity flow column and elution by 20 mM Tris-HCl pH 7.5, 500 mM KCl, 7,5% glycerol, 300 mM

imidazole, and 1 mM DTT. Obtained proteins were dialysed against cleavage buffer (CB), comprising 20 mM Tris-HCl (pH 7.5), 250 mM KCl, 7,5% glycerol, 1 mM DTT. Then peptide bond hydrolysis was carried out with 6xhis-labeled peptidase Ulp1 in CB. Hydrolysis was carried out during the night at +4 º. Then mix was incubated with Ni-NTA agarose, equilibrated in CB, and purified using gravity flow column. The product was dialysed in storage buffer (SB): 20 mM Tris-HCl (pH 7.5), 100 mM KCl, 10% glycerol, 1 mM DTT, frizzed in liquid nitrogen and stored at -70º. The composition of CB for Nsp1 C domain (~4,8 kDa) was identical with SB and the dialysis was not carried out.

Cloning for readthrough assay

pNL-globine construct was kindly provided by Ilia Terenin. pNL-globine vector was amplified by PCR with Q5 polymerase (NEB) using primers pNL_F and pNL-gl_R. Stop codons with the weak 3' context, as well as positive controls, were made using corresponding primers (Table 1). Obtained sequences were cloned into pNL-globine vector using Gibson Assembly® Master Mix (NEB), Gibson Assembly® Master Mix (NEB)

Table 1. Primers used.

NSP1_F	GAGAACAGATTGGTGGTATGGAGAGCCTGGTGCCTG
NSP1_R	CCGAATAAATACCTAAGCTTAGCCACCGTTCAGTTCACGC
petSUMO_F	AGCTTAGGTATTTATTCGGCGCAAAGTG
petSUMO_R	ACCACCAATCTGTTCTCTGTGAGC
ΔNSP1_F	GAGAACAGATTGGTGGTCACGTGCAGCTGTCTCTGCC
NSP1_N_R	CCGAATAAATACCTAAGCTTAAGCACCGTAGGAGTGTCCG
NSP1_C_F	GAGAACAGATTGGTGGTGACCTGAAGTCTTTCGACCTGGGC
RK/SE_F	TACAGAAAGGTGCTGCTGAGTGAGAACGGAAACAAGGGTG
RK/SE_R	CACCCTTGTTTCCGTTCTCACTCAGCAGCACCTTTCTGTA
NK/SE_F	GCTGCTGCGTAAGAACGGAAGCGAGGGTGCCGGC
NK/SE_R	GCCGGCACCCTCGCTTCCGTTCTTACGCAGCAGC
NSP1_KH/AA_	CAGGAAAACTGGAACACCGCGGCCAGCTCCGGAGTGACCAG
NSP1_KH/AA_	CTGGTCACTCCGGAGCTGGCCGCGGTGTTCCAGTTTTCCTG

NSP1_YF/AA_	ACGAGCTGGGAACTGACCCTGCCGAGGACGCCCAGGAAAACTGGAAC
NSP1_YF/AA_	GTTCCAGTTTTCCTGGGCGTCCTCGGCAGGGTCAGTTCCCAGCTCGT
NSP1_RR/EE_F	GCACAGCTCCGGAGTGACCGAGGAGCTGATGGAGGAACTGAACGGTGGCTAAG
NSP1_RR/EE_	CTTAGCCACCGTTCAGTTCCTCCATCAGCTCCTCGGTCACTCCGGAGCTGTGC
3xFLAG_F	GAGAACAGATTGGTGGTGACTACAAAGACCATGACGGTGAT
3xFLAG_R	ACCAGGCTCTCCATCTTATCGTCGTCGTCCTTGTAATC
pNL_F	ATAGTCTTCACACTCGAAGATTTCGTTG
pNL-gl_R	GGTGTCTGTTTTGGGGGATTG
UAA_G-rich_F	CCCAAAACAGACACCATGGTGCATCTGACTCCTGAGGAGAAGTCTGCCGTTACTT
UAA_G-rich_R	CTTCGAGTGTGAAGACTATGGTCAGCCCTTAAGTAACGGCAGACTTCTCCTCAGGA
AAA_G-rich_F	CCCAAAACAGACACCATGGTGCATCTGACTCCTGAGGAGAAGTCTGCCGTTACTA
AAA_G-rich_R	CTTCGAGTGTGAAGACTATGGTCAGCCCTTTAGTAACGGCAGACTTCTCCTCAGGA
UAG_Dyst_F	CCCAAAACAGACACCATGGTGCATCTGACTCCTGAGGAGAAGTCTGCCGTTAC
UAG_Dyst_R	CTTCGAGTGTGAAGACTATGGTATTATCCTAAGTAACGGCAGACTTCTCCTCAGGA
UAU_Dyst_F	CCCAAAACAGACACCATGGTGCATCTGACTCCTGAGGAGAAGTCTGCCGTTACTT
UAU_Dyst_R	CTTCGAGTGTGAAGACTATGGTATTATCATAAGTAACGGCAGACTTCTCCTCAGGA
UGA_weak1_F	CCCAAAACAGACACCATGGTGCATCTGACTCCTGAGGAGAAGTCTGCCGTTACTT
UGA_weak1_R	CTTCGAGTGTGAAGACTATGGTTACTAGTCAAGTAACGGCAGACTTCTCCTCAGGA
UGU_weak1_F	CCCAAAACAGACACCATGGTGCATCTGACTCCTGAGGAGAAGTCTGCCGTTACTT
UGU_weak1_R	CTTCGAGTGTGAAGACTATGGTTACTAGACAAGTAACGGCAGACTTCTCCTCAGG

Pre-termination complex assembly

The 40S and 60S ribosomal subunits as well as eukaryotic translation factors eIF2, eIF3, eEF1H, and eEF2 were purified from RRL or HeLa lysate, as previously described (Alkalaeva et al., 2006). The human translation factors eIF1, eIF1A, eIF4A, eIF4B, ΔeIF4G, ΔeIF5B, eIF5, PABP, and eRF1 were produced as recombinant proteins in *E. coli* strain BL21 with subsequent protein purification on Ni-NTA agarose and ion-exchange chromatography (Alkalaeva et al., 2006). Human eRF3a was

expressed in insect Sf21 cells and purified via affinity chromatography using a HisTrap HP column (GE Healthcare) followed by anion-exchange chromatography using a MonoQ column (GE Healthcare) (Ivanov et al., 2016). mRNAs were transcribed *in vitro* (T7 RiboMAX Express Large Scale RNA Production System, Promega, USA) from the linear fragment of the pET28-MVHL-UAA plasmid containing the T7 promoter, four CAA repeats, β-globin 5'-UTR, and ORF (encoding for the peptide MVHL), followed by the stop codon UAA and 3'-UTR, comprising the remaining natural β-globin coding sequence. Eukaryotic preTCs on MVHL-UAA mRNA were assembled and purified as previously described (Alkalaeva et al., 2006; Egorova et al., 2019; Mikhailova et al., 2017). Briefly, ribosomal complexes were assembled in a 500 μL solution containing 37 pmol of mRNA. They were incubated for 15 min in buffer A (20 mM Tris acetate (pH 7.5), 100 mM KAc, 2.5 mM $MgCl_2$, 2 mM DTT) supplemented with 400 U RiboLock RNase inhibitor (Thermo Fisher Scientific, cat# EO0384), 1 mM ATP, 0.25 mM spermidine, 0.2 mM GTP, 75 μg calf liver total tRNA (acylated with all or individual amino acids; Sigma, cat# R7250), 75 pmol human 40S and 60S purified ribosomal subunits, 200 pmol eIF2, 60 pmol eIF3, 400 pmol eIF4A, 150 pmol eIF4B, and 125 pmol each of human eIF2, ΔeIF4G, eIF1, eIF1A, eIF5, and ΔeIF5B for the formation of the 80S initiation complex. After 15 min, 200 pmol of human eEF1H and 38 pmol of eEF2 were added to form the elongation complex. The ribosomal complexes were then purified via centrifugation in a Beckman SW55 rotor for 95 min at 4 °C and 48,000 rpm in a 10–30% (w/w) linear sucrose density gradient (SDG) prepared in buffer A with 5 mM $MgCl_2$. Fractions corresponding to the ribosomal complexes were diluted three-fold with buffer A containing 1.25 mM $MgCl_2$ (to a final concentration of 2.5 mM Mg^{2+}) and used in experiments.

Termination complex (TC) formation efficiency assay

First, 0.03 pmol preTCs incubated with release factors (0.5 pmol eRF1/eRF1(AGQ) alone or 0.1 pmol eRF1/eRF1(AGQ) with 0.1 pmol eRF3a) and optionally with 2.5 pmol Nsp1 or its mutants/domains or eIF1A as negative control at 37 °C for 15 min in the presence of 0.2 mM GTP or GDPCP, supplemented with equimolar amounts of $MgCl_2$. Samples were analysed using the primer extension protocol. The toe-printing analysis was performed with AMV reverse transcriptase and 5'-carboxyfluorescein-labelled primers complementary to 3'-UTR sequences, as described previously (Egorova et al., 2019). cDNAs were separated via electrophoresis using standard GeneScan® conditions on an ABI Prism® Genetic Analyser 3100 (Applera). Chromatograms were visualized in GeneMarker v. 1.5 (SoftGenetics LLC).

Termi-Luc peptide release assay

A peptide release with Nanoluciferase (NLuc) was performed as previously described (Susorov et

al., 2020) with modifications. The assay allows measurement of the NLuc release from TCs assembled on NLuc mRNA in RRL. NLuc folds into the catalytically active form only after its release from the ribosome, which leads to luminescence in the presence of substrate. The NanoLuc mRNA was *in vitro* transcribed (T7 RiboMAX Express Large Scale RNA Production System, Promega, USA) from a template containing β-globin 5'-UTR, NLuc CDS, 3'-UTR derived from pNL1.1[Nluc] vector (Promega), and 50 nt poly(A) tail. 1 ml of RRL lysate (Green Hectares, USA) was preincubated in a mixture containing 1.5 u/µl Micrococcal nuclease (Fermentas) and 1 mM $CaCl_2$ at 30°C for 10 min, followed by the addition of EGTA to a final concentration of 2 mM. A reaction mixture containing 70% nuclease-treated RRL was supplemented with 20 mM Hepes-KOH (pH 7.5), 80 mM KOAc, 0.5 mM $Mg(OAc)_2$, 0.36 mM ATP, 0.2 GTP, 0.05 mM each of 20 amino acids (Promega), 0.5 mM spermidine, 5 ng/µl total deacylated rabbit tRNAs, 10 mM creatine phosphate, 0.003 u/µl creatine kinase (Sigma), 2 mM DTT and 0.2 U/µl Ribolock (ThermoFisher) in a volume of 1 ml. The mixture was preincubated with 1 µM eRF1(AGQ) at 30°C for 10 min, followed by the addition of the NLuc mRNA to a final concentration of 8 µg/ml, resulting in the formation of TCs. Next, KOAc concentration was adjusted to 300 mM and the mixture was layered on 10–35% linear sucrose gradient in buffer containing 50 mM Hepes-KOH, pH 7.5, 7.5 mM $Mg(OAc)_2$, 300 mM KOAc, 2 mM DTT. The gradients were centrifuged in a SW-41 Ti (Beckman Coulter) rotor at 18000 rpm for 14 h. Fractions enriched with preTCs were collected. PreTC was aliquoted, flash-frozen in liquid nitrogen, and stored at −80 °C. Peptide release was performed in solution containing 8 nM preTC, 50 mM Hepes-KOH, pH 7.5, 0.25 mM spermidine, 2 mM DTT, 0.2 mM GTP, and 1% NLuc substrate (Nano-Glo, Promega) in the presence of release factors (4 nM eRF1 alone or with 4 nM eRF3a) and 80µM Nsp1 protein or its mutants/domains or eIF1A as negative control. When testing the effect of antibiotics, gentamicin (Sigma) or mephloquine (Sigma) were additionally added to a final concentration of 100 µM. Luminescence was measured for 1 hour at 30°C using a Tecan Infinite 200Pro (Tecan, Männedorf, Switzerland). The peptide release kinetic curves or histogram with maximum values were generated and the standard deviation was calculated in Microsoft Excel.

In vitro translation assay

For the *in vitro* translation the Nano-Luc mRNAs were used (Table 2). Each mRNA contained β-globin 5'-UTR, coding sequence of first 13 aminoacids of β–globin with or without different premature termination codons (PTC) followed by the different 3' hexanucleotide weak contexts (Table 2), NLuc CDS, 3'-UTR derived from pNL1.1[Nluc] vector (Promega), and 50 nt poly(A) tail. mRNAs were in vitro transcribed (T7 RiboMAX Express Large Scale RNA Production System, Promega, USA) from the pNL-globine templates described above.

Table 2. mRNAs used in *in vitro* translation assay

sequence	**weak context**	**mRNA name**
UGUCUAGUA	weak (Loughran et al., 2014)	NLuc-UGU mRNA
UGACUAGUA		NLuc-UGA mRNA
UAUGAUAAU	dystrophine (Bidou et al., 2004)	NLuc-UAU mRNA
UAGGAUAAU		NLuc-UAG mRNA
AAAGGG CUG	G-rich (Sokolova et al., 2020)	NLuc-AAA mRNA
UAAGGG CUG		NLuc-UAA mRNA

premature termination codon (PTC) in bold

The translation was performed in nuclease-treated RRL obtained as described above. Translation mixture contained 70% nuclease-treated RRL was supplemented with 20 mM Hepes-KOH (pH 7.5), 80 mM KOAc, 0.5 mM $Mg(OAc)_2$, 0.36 mM ATP, 0.2 GTP, 0.05 mM each of 20 amino acids (Promega), 0.5 mM spermidine, 5 ng/µl total deacylated rabbit tRNAs, 10 mM creatine phosphate, 0.003 u/µl creatine kinase (Sigma), 2 mM DTT, 0.2 U/µl Ribolock (ThermoFisher), 1% NLuc substrate (Nano-Glo, Promega), 16 pg/µl NLuc-mRNA and 0.6 µM Nsp1 protein or its mutants/domains or eIF1A as negative control. Luminescence was measured at 30°C during 1 h uusing a Tecan Infinite 200 Pro (Tecan, Männedorf, Switzerland). For the translation efficiency experiments, NLuc-UGU mRNA was used. The data was presented as luminescence time progress curve with standards deviations, plotted in Microsoft Excel. PTC readthrough was calculated using the formula: (maximum luminescence of the PTC-luc mRNA/maximum luminescence of the luc mRNA)*100%.

GTPase assay

Ribosomal 40S and 60S subunits (5 pmol each) with 5 pmol of eRF1 were associated at 37 °C for 10 min. Then, other components were added. Final reaction volume was 10 µL and contained 23.5 mM Tris-HCl pH 7.5, 35 mM NH_4Cl, 18 mM $MgCl_2$, 0.5 mM GTP, 3 pmol of eRF3a and 0, 3, 5, 10 or 15 pmol of Nsp1. After incubation for 15 min at 37 °C the amount of released phosphate was estimated with Malachite Green Phosphate Assay (Sigma), according to the manufacturer's protocol.

QUANTIFICATION AND STATISTICAL ANALYSIS

All experiments were carried out in at least 3 replicates (the specific number of replicates is shown in the description under figures). The data is presented as mean±standard deviation (SD), when analyzing luminescence signals of lysates, or mean±standard error of mean (SE), when analyzing parameters (translation and readthrough efficiency). A two-tailed t-test was used to compare mean values between two groups. For multiple comparisons, the Bonferroni correction was used. One-way ANOVA was used to compare mean values between more than two groups.

P-values were calculated in Microsoft Excel. The difference was considered significant when p was less than 0.05 (Glantz, 2011).

SUPPLEMENTARY DATA

Supplementary Data are available at

ACKNOWLEDGEMENT

We are grateful to Ludmila Frolova for providing plasmids encoding release factors and to Tatyana Pestova and Christopher Hellen who provided us with plasmids encoding initiation factors. pDONR207 SARS-CoV-2 NSP1 was a kind gift from Fritz Roth (Addgene plasmid # 141255; http://n2t.net/addgene:141255; RRID: Addgene_141255). Sequencing of plasmids, coding mutant proteins and cDNA fragment analyses were performed by the equipment of EIMB RAS "Genome" center (http://www.eimb.ru/ru1/ckp/ccu_genome_c.php).

FUNDING

This work was supported by the grant 075-15-2019-1660 from the Ministry of Science and Higher Education of the Russian Federation.

CONFLICT OF INTEREST

None declared.

REFERENCES

Alkalaeva, E.Z., Pisarev, A. V., Frolova, L.Y., Kisselev, L.L., and Pestova, T. V. (2006). In Vitro Reconstitution of Eukaryotic Translation Reveals Cooperativity between Release Factors eRF1 and eRF3. Cell 125, 1125–1136.

Banerjee, A.K., Blanco, M.R., Bruce, E.A., Honson, D.D., Chen, L.M., Chow, A., Bhat, P., Ollikainen, N., Quinodoz, S.A., Loney, C., et al. (2020). SARS-CoV-2 Disrupts Splicing, Translation, and Protein Trafficking to Suppress Host Defenses. Cell.

Bidou, L., Hatin, I., Perez, N., Allamand, V., Panthier, J., and Rousset, J. (2004). Premature stop codons involved in muscular dystrophies show a broad spectrum of readthrough efficiencies in response to gentamicin treatment. Gene Ther. 11, 619–627.

Brown, A., Shao, S., Murray, J., Hegde, R.S., and Ramakrishnan, V. (2015). Structural basis for stop codon recognition in eukaryotes. Nature 524, 493–496.

Cheng, Z., Saito, K., Pisarev, A. V., Wada, M., Pisareva, V.P., Pestova, T. V., Gajda, M., Round, A., Kong, C., Lim, M., et al. (2009). Structural insights into eRF3 and stop codon recognition by eRF1. Genes Dev. 23, 1106–1118.

Egorova, T., Sokolova, E., Shuvalova, E., Matrosova, V., Shuvalov, A., and Alkalaeva, E. (2019). Fluorescent toeprinting to study the dynamics of ribosomal complexes. Methods 162–163, 54–59.

Ferguson, M.W., Gerak, C.A.N., Chow, C.C.T., Rastelli, E.J., Elmore, K.E., Stahl, F., Hosseini-Farahabadi, S., Baradaran-Heravi, A., Coltart, D.M., and Roberge, M. (2019). The antimalarial drug mefloquine enhances TP53 premature termination codon readthrough by aminoglycoside G418. PLoS One 14, 1–15.

Frolova, L., Le Goff, X., Rasmussen, H.H., Cheperegin, S., Drugeon, G., Kress, M., Arman, I., Haenni, A.-L., Celis, J.E., Phllippe, M., et al. (1994). A highly conserved eukaryotic protein family possessing properties of polypeptide chain release factor. Nature 372, 701–703.

Frolova, L., Le Goff, X., Zhouravleva, G., Davydova, E., Philippe, M., and Kisselev, L. (1996). Eukaryotic polypeptide chain release factor eRF3 is an eRF1- and ribosome-dependent guanosine triphosphatase. RNA 2, 334–341.

Frolova, L.Y., Tsivkovskii, R.Y., Sivolobova, G.F., Oparina, N.Y., Serpinsky, O.I., Blinov, V.M., Tatkov, S.I., and Kisselev, L.L. (1999). Mutations in the highly conserved GGQ motif of class I polypeptide release factors abolish ability of human eRF1 to trigger peptidyl-tRNA hydrolysis. Rna 5, 1014–1020.

Glantz, S.A. (2011). Primer of Biostatistics (McGraw-Hill Education / Medical).

Ivanov, A., Mikhailova, T., Eliseev, B., Yeramala, L., Sokolova, E., Susorov, D., Shuvalov, A.,

Schaffitzel, C., and Alkalaeva, E. (2016). PABP enhances release factor recruitment and stop codon recognition during translation termination. Nucleic Acids Res. 44, 7766–7776.

Jackson, R.J., Hellen, C.U.T., and Pestova, T. V. (2012). Termination and post-termination events in eukaryotic translation. In Advances in Protein Chemistry and Structural Biology, (Academic Press), pp. 45–93.

Kamitani, W., Huang, C., Narayanan, K., Lokugamage, K.G., and Makino, S. (2009). A two-pronged strategy to suppress host protein synthesis by SARS coronavirus Nsp1 protein. Nat. Struct. Mol. Biol. 16, 1134–1140.

Kim, D.-K., Knapp, J.J., Kuang, D., Chawla, A., Cassonnet, P., Lee, H., Sheykhkarimli, D., Samavarchi-Tehrani, P., Abdouni, H., Rayhan, A., et al. (2020a). A Comprehensive, Flexible Collection of SARS-CoV-2 Coding Regions. G3 Genes, Genomes, Genet. 10, 3399–3402.

Kim, D., Lee, J.Y., Yang, J.S., Kim, J.W., Kim, V.N., and Chang, H. (2020b). The Architecture of SARS-CoV-2 Transcriptome. Cell 181, 914-921.e10.

Kryuchkova, P., Grishin, A., Eliseev, B., Karyagina, A., Frolova, L., and Alkalaeva, E. (2013). Two-step model of stop codon recognition by eukaryotic release factor eRF1. Nucleic Acids Res. 41, 4573–4586.

Lapointe, C.P., Grosely, R., Johnson, A.G., Wang, J., Fernández, I.S., and Puglisi, J.D. (2020). Dynamic competition between SARS-CoV-2 NSP1 and mRNA on the human ribosome inhibits translation initiation. BioRxiv 2020.08.20.259770.

Loughran, G., Chou, M.Y., Ivanov, I.P., Jungreis, I., Kellis, M., Kiran, A.M., Baranov, P. V., and Atkins, J.F. (2014). Evidence of efficient stop codon readthrough in four mammalian genes. Nucleic Acids Res. 42, 8928–8938.

Matheisl, S., Berninghausen, O., Becker, T., and Beckmann, R. (2015). Structure of a human translation termination complex. Nucleic Acids Res. 43, 8615–8626.

Mikhailova, T., Shuvalova, E., Ivanov, A., Susorov, D., Shuvalov, A., Kolosov, P.M., and Alkalaeva, E. (2017). RNA helicase DDX19 stabilizes ribosomal elongation and termination complexes. Nucleic Acids Res. 45, 1307–1318.

Prokhorova, I., Altman, R.B., Djumagulov, M., Shrestha, J.P., Urzhumtsev, A., Ferguson, A., Chang, C.W.T., Yusupov, M., Blanchard, S.C., Yusupova, G., et al. (2017). Aminoglycoside interactions and impacts on the eukaryotic ribosome. Proc. Natl. Acad. Sci. U. S. A. 114, E10899–E10908.

Schubert, K., Karousis, E.D., Jomaa, A., Scaiola, A., Echeverria, B., Gurzeler, L.-A., Leibundgut, M., Thiel, V., Mühlemann, O., and Ban, N. (2020). SARS-CoV-2 Nsp1 binds the ribosomal mRNA channel to inhibit translation. Nat. Struct. Mol. Biol. 27, 959–966.

Shao, S., Murray, J., Brown, A., Taunton, J., Ramakrishnan, V., and Hegde, R.S. (2016). Decoding Mammalian Ribosome-mRNA States by Translational GTPase Complexes. Cell 167, 1229-1240.e15.

Shi, M., Wang, L., Fontana, P., Vora, S., Zhang, Y., Fu, T.-M., Lieberman, J., and Wu, H. (2020). SARS-CoV-2 Nsp1 suppresses host but not viral translation through a bipartite mechanism. BioRxiv 2, 2020.09.18.302901.

Sokolova, E.E., Vlasov, P.K., Egorova, T.V., Shuvalov, A.V., and Alkalaeva, E.Z. (2020). The Influence of A/G Composition of 3' Stop Codon Contexts on Translation Termination Efficiency in Eukaryotes. Mol. Biol. (Mosk). 54.

Song, H., Mugnier, P., Das, A.K., Webb, H.M., Evans, D.R., Tuite, M.F., Hemmings, B.A., and Barford, D. (2000). The Crystal Structure of Human Eukaryotic Release Factor eRF1—Mechanism of Stop Codon Recognition and Peptidyl-tRNA Hydrolysis. Cell 100, 311–321.

Susorov, D., Egri, S., and Korostelev, A.A. (2020). Termi-Luc: a versatile assay to monitor full-protein release from ribosomes. RNA rna.076588.120.

Taylor, D., Unbehaun, A., Li, W., Das, S., Lei, J., Liao, H.Y., Grassucci, R.A., Pestova, T. V., and Frank, J. (2012). Cryo-EM structure of the mammalian eukaryotic release factor eRF1-eRF3-associated termination complex. Proc. Natl. Acad. Sci. 109, 18413–18418.

Thoms, M., Buschauer, R., Ameismeier, M., Koepke, L., Denk, T., Hirschenberger, M., Kratzat, H., Hayn, M., Mackens-Kiani, T., Cheng, J., et al. (2020). Structural basis for translational shutdown and immune evasion by the Nsp1 protein of SARS-CoV-2. Science (80-.). 369, 1249–1255.

Tidu, A., Schaeffer, L., Sosnowski, P., Kuhn, L., Hammann, P., Westhof, E., Eriani, G., Martin, F., Mol, B., Upr, C., et al. (2020). The viral protein NSP1 acts as a ribosome gatekeeper for shutting down host translation and fostering SARS-CoV-2 translation. BioRxiv 10.1101, 2020.10.14.339515.

Wilhelm, J.M., Pettitt, S.E., and Jessop, J.J. (1978). Aminoglycoside antibiotics and eukaryotic protein synthesis: structure-function relationships in the stimulation of misreading with a wheat embryo system. Biochemistry 17, 1143–1149.

Wong, W., Bai, X.C., Sleebs, B.E., Triglia, T., Brown, A., Thompson, J.K., Jackson, K.E., Hanssen, E., Marapana, D.S., Fernandez, I.S., et al. (2017). Mefloquine targets the Plasmodium falciparum 80S ribosome to inhibit protein synthesis. Nat. Microbiol. 2.

Wu, A., Peng, Y., Huang, B., Ding, X., Wang, X., Niu, P., Meng, J., Zhu, Z., Zhang, Z., Wang, J., et al. (2020). Genome Composition and Divergence of the Novel Coronavirus (2019-nCoV) Originating in China. Cell Host Microbe 27, 325–328.

Xia, H., Cao, Z., Xie, X., Zhang, X., Chen, J.Y.C., Wang, H., Menachery, V.D., Rajsbaum, R., and Shi, P.Y. (2020). Evasion of Type I Interferon by SARS-CoV-2. Cell Rep. 33, 108234.

Yuan, S., Peng, L., Park, J.J., Hu, Y., Devarkar, S.C., Dong, M.B., Shen, Q., Wu, S., Chen, S., Lomakin, I.B., et al. (2020). Nonstructural protein 1 of SARS-CoV-2 is a potent pathogenicity factor redirecting host protein synthesis machinery toward viral RNA. Mol. Cell 2020.08.09.243451.

Zhou, P., Yang, X. Lou, Wang, X.G., Hu, B., Zhang, L., Zhang, W., Si, H.R., Zhu, Y., Li, B., Huang, C.L., et al. (2020). A pneumonia outbreak associated with a new coronavirus of probable bat origin. Nature 579, 270–273.

Zhu, N., Zhang, D., Wang, W., Li, X., Yang, B., Song, J., Zhao, X., Huang, B., Shi, W., Lu, R., et al. (2020). A novel coronavirus from patients with pneumonia in China, 2019. N. Engl. J. Med. 382, 727–733.

TABLE AND FIGURES LEGENDS

Figure 1. Nsp1 activates peptidyl-tRNA hydrolysis with the release factors. (A) *In vitro* Nluc mRNA translation in RRL in presence/absence of Nsp1. Time progress curves showing luminescence (in relative luminescence units, rlu), n=3, mean±SD (B) Termi-Luc peptide release assay in presence/absence of Nsp1 and the release factors. Time progress curves showing luminescence (in relative luminescence units, rlu) with NLuc released from ribosome complex upon treatment with the proteins of interest. eIF1A was added to the reaction as a negative control. n=3, mean±SD

Figure 2. Nsp1 stimulates TC formation with the release factors. (A) An example of raw toe-printing data. PreTC were purified by sucrose density gradient centrifugation; TC formation was induced by the addition of eRF1/eRF1(AGQ) and Nsp1 or eIF1A as a negative control. (B) TC formation induced by the addition of eRF1+eRF3a/eRF1(AGQ)+eRF3a and Nsp1 or eIF1A as a negative control. The TC corresponds to the black triangle, and the preTC corresponds to the white triangle. Red stars indicate the increased quantity of ribosomal complexes, shifted from the preTC to the TC state.

Figure 3. (A) GTPase activity of the eRF3a in the presence of the ribosome subunits, eRF1 and Nsp1, n=4, mean±SE, n.s. – not significant (B) Nsp1 stimulation of TC formation does not depend on GTP hydrolysis. An example of raw toe-printing data. TC formation was induced by the addition of eRF1+eRF3a+GDPCP and Nsp1 or eIF1A as a negative control. The TC corresponds to the black triangle, and the preTC corresponds to the white triangle. Red stars indicate the increased quantity of ribosomal complexes, shifted from the preTC to the TC state. (C) Termi-Luc peptide release assay in the presence/absence of Nsp1 and NM domain of eRF1. Time progress curves showing luminescence (in relative luminescence units, rlu) with NLuc released from the ribosome complex upon treatment with the proteins of interest, n=3, mean±SD

Figure 4. (A) Scheme of the Nsp1 constructions used in the experiments: Nsp1 N/C domains and Nsp1 mutants (B) *In vitro* Nluc mRNA translation in RRL in the presence/absence of Nsp1 mutants and ΔNsp1. Time progress curves showing luminescence (in relative luminescence units, rlu) (C) Termi-Luc peptide release assay in the presence/absence of Nsp1 mutants, ΔNsp1, and the release factors. Time progress curves showing luminescence (in relative luminescence units, rlu) with NLuc released from the ribosome complex upon treatment with the proteins of interest., n=3, mean±SD

Figure 5. (A) *In vitro* Nluc mRNA translation in RRL in the presence/absence N/C domains of Nsp1, n=3, mean±SD (B) Termi-Luc peptide release assay in the presence/absence of N/C domains of Nsp1 and the release factors. Time progress curves showing luminescence (in relative luminescence units, rlu) with NLuc released from the ribosome complex upon treatment with the proteins of interest. The number of replicates is three. The error bars represent the standard mean deviation, n=3, mean±SD (C) An example of raw toe-printing data. TC formation was induced by the addition of eRF1 or eRF1+eRF3a and Nsp1 or N/C domains of Nsp1. An addition of eIF1A was used as a negative control. The TC corresponds to the black triangle, and the preTC corresponds to the white triangle. Red stars indicate the increased quantity of ribosomal complexes, shifted from the preTC to the TC state.

Figure 6. Nsp1 affected PTC readthrough in RRL. (A) Scheme of the NLuc constructions containing the leaking contexts in β-globine 5' UTR followed by sense codon or PTC. (B) *In vitro* translation in RRL with Nluc mRNA containing sense codons or PTCs in the presence/absence Nsp1 and Nsp1 mutant - KH/AA, relative luminescence units (rlu). n=4, 3, 3, respectively, mean±SE, * - $p<0.05$, ** - $p<0.01$. (C) An example of raw toe-printing data. TC formation was induced by the addition of eRF1+eRF3a in presence of Nsp1 on different stop codons. The TC corresponds to the black triangle, and the preTC corresponds to the white triangle. Red stars indicate the increased quantity of ribosomal complexes, shifted from the preTC to the TC state.

Figure 7. Gentamicin and mefloquine influence on Nsp1-mediated termination stimulation. (A) Termi-Luc peptide release assay in the presence/absence of Nsp1 and gentamicin or mefloquine with the release factors. Maximum luminescence values of NLuc released from the ribosome complex upon treatment in relative luminescence units, rlu. n=3, mean±SE, n.s. – not significant, * - $p<0.05$ (B) An example of raw toe-printing data. TC formation was induced by the addition of eRF1 or eRF1+eRF3a with GTP or GTPCP, gentamicin (Gm)/mefloquine (MFQ), and Nsp1. An addition of eIF1A was used as a negative control. The TC corresponds to the black triangle, and the preTC corresponds to the white triangle. Red stars indicate the increased quantity of ribosomal complexes, shifted from the preTC to the TC state.

SUPPLEMENTARY DATA

Figure S1. (A) An example of raw toe-printing data. TC formation was induced by the addition of eRF1 or eRF1+eRF3a and Nsp1 or six different Nsp1 mutants. An addition of eIF1A was used as a negative control. The TC corresponds to the black triangle, and the preTC corresponds to the white triangle. Red stars indicate the increased quantity of ribosomal complexes, shifted from the preTC to the TC state.

Figure S2. (A) *In vitro* Nluc mRNA translation in RRL in the presence/absence of 3xFLAG-Nsp1. Time progress curves showing luminescence (in relative luminescence units, rlu), n=3, mean±SD (B) Termi-Luc peptide release assay in the presence/absence of 3xFLAG-Nsp1 and the release factors. Time progress curves showing luminescence (in relative luminescence units, rlu) with NLuc released from the ribosome complex upon treatment with the protein of interest, n=3, mean±SD (C) An example of raw toe-printing data. TC formation was induced by the addition of eRF1 or eRF1+eRF3a+GTP and Nsp1 or 3×FLAG-Nsp1. An addition of eIF1A was used as a negative control. The TC corresponds to the black triangle, and the preTC corresponds to the white triangle. Red stars indicate the increased quantity of ribosomal complexes, shifted from the preTC to the TC state.

A

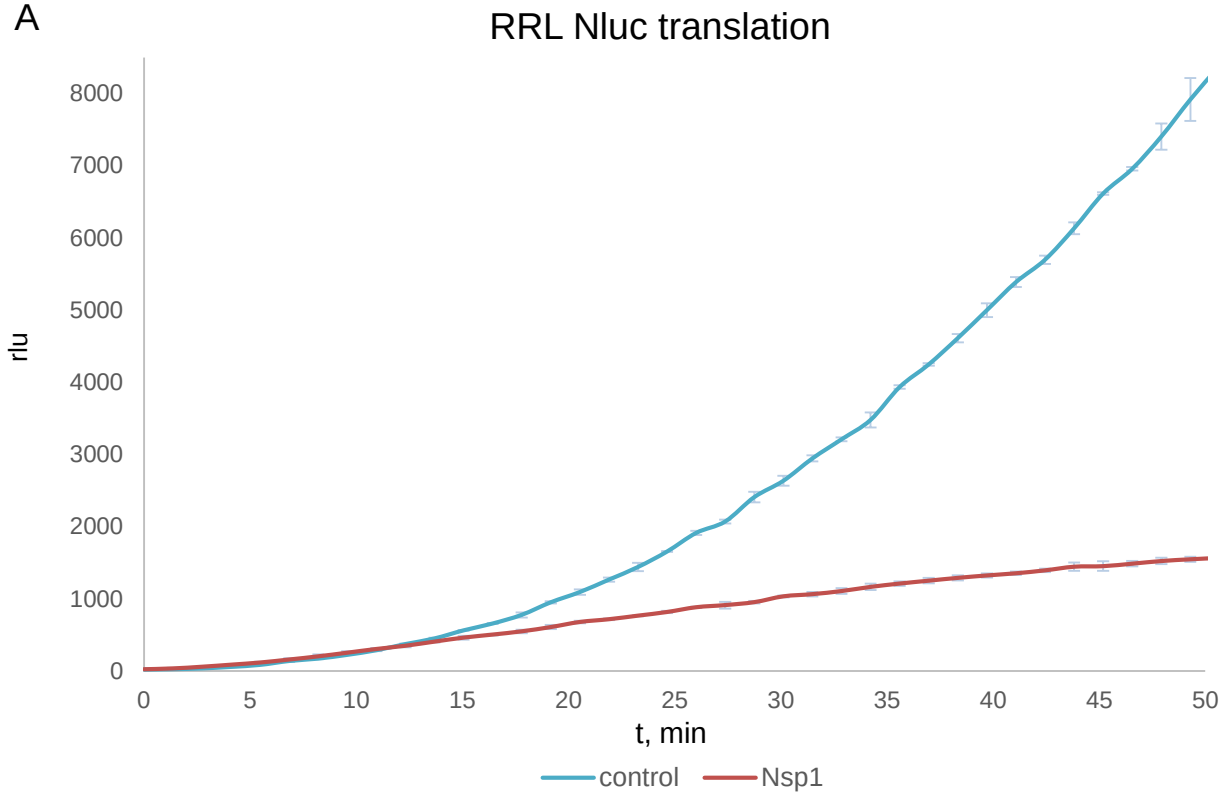
RRL Nluc translation
rlu
8000
7000
6000
5000
4000
3000
2000
1000
0
0
5
10
15
20
25
30
35
40
45
50
t, min
control
Nsp1

B

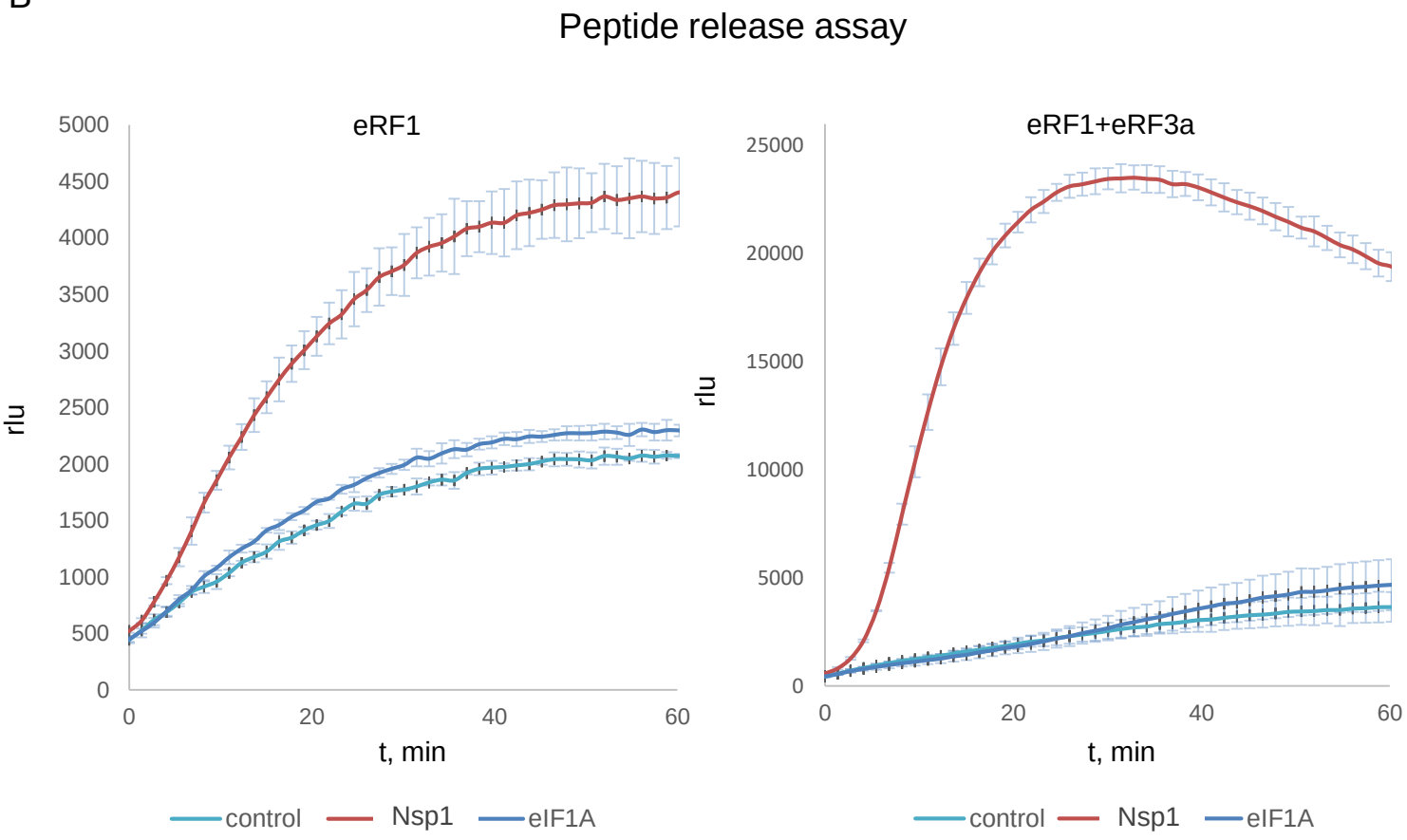
Peptide release assay
eRF1
rlu
5000
4500
4000
3500
3000
2500
2000
1500
1000
500
0
0
20
40
60
t, min
control
Nsp1
eIF1A
eRF1+eRF3a
rlu
25000
20000
15000
10000
5000
0
0
20
40
60
t, min
control
Nsp1
eIF1A

Fig 1

A Toe printing assay

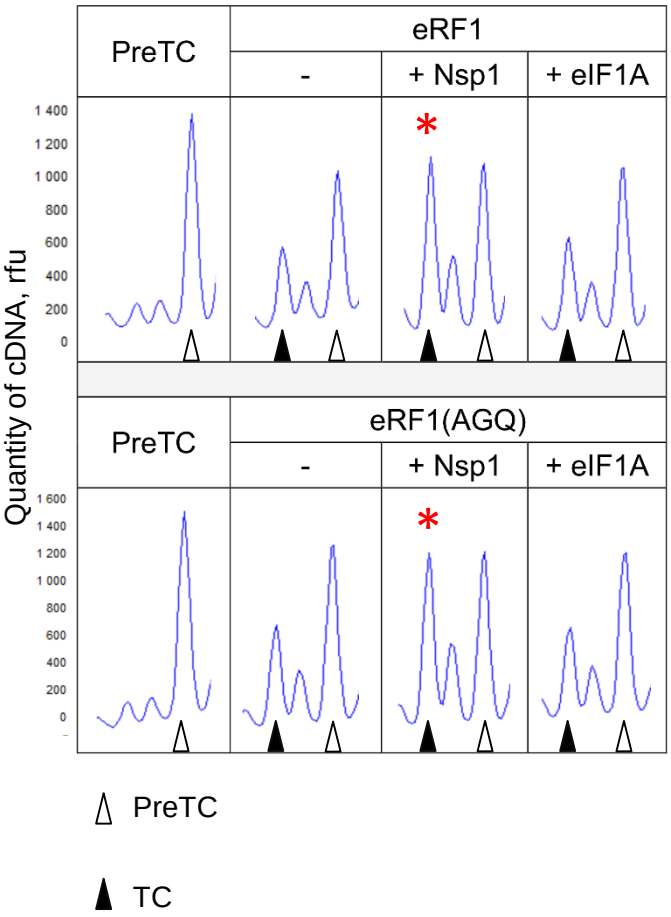

PreTC

TC

B Toe printing assay

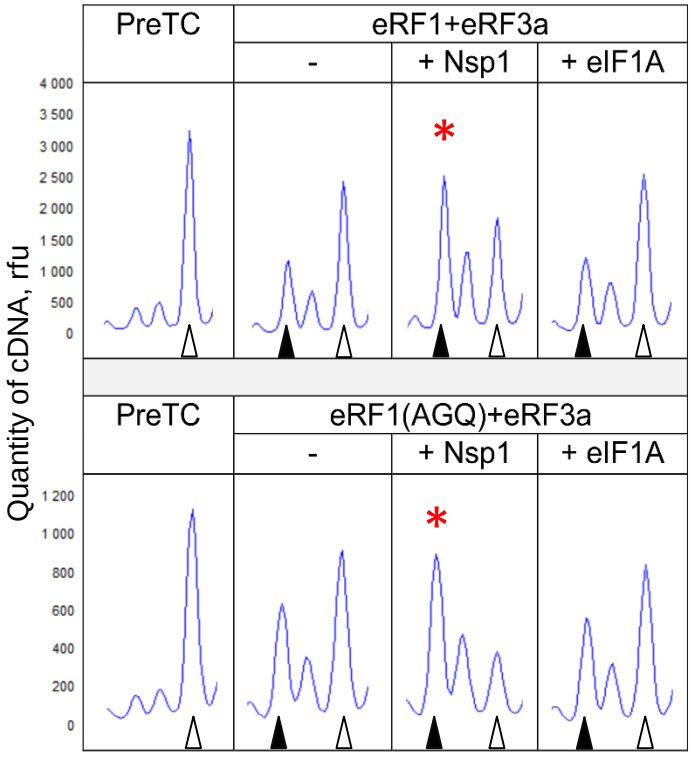

Fig 2

A

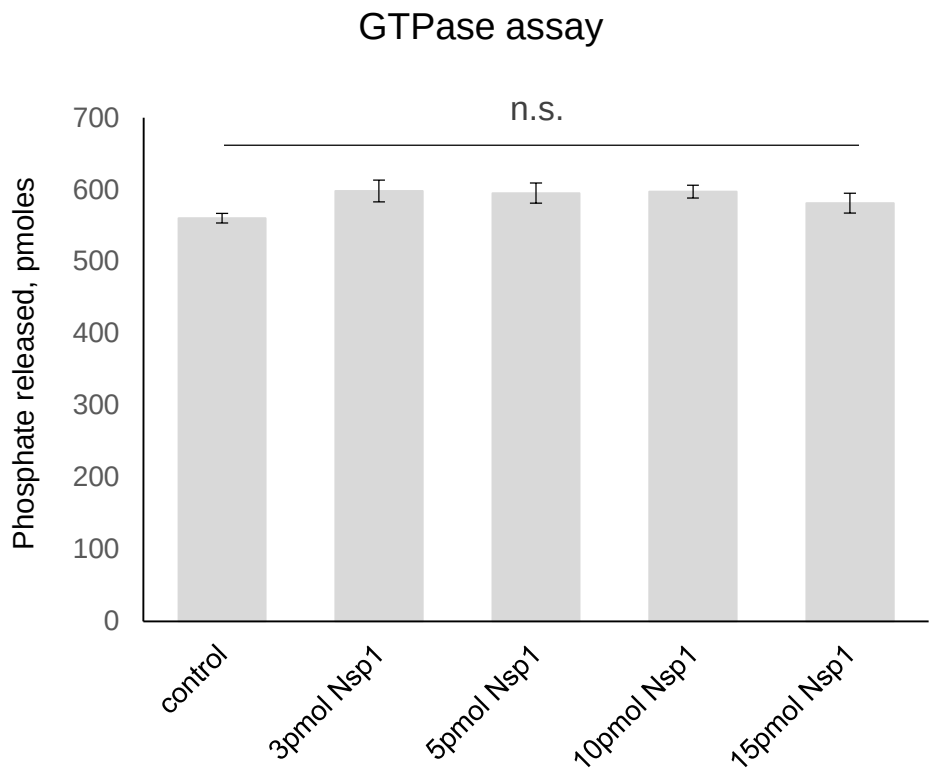
GTPase assay
n.s.
Phosphate released, pmoles
700
600
500
400
300
200
100
0
control
3pmol Nsp1
5pmol Nsp1
10pmol Nsp1
15pmol Nsp1

B

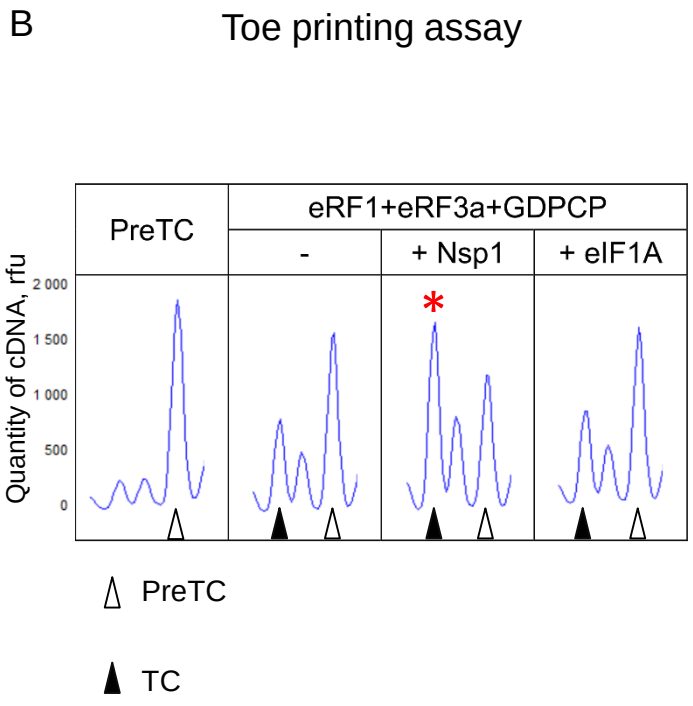
Toe printing assay
PreTC
eRF1+eRF3a+GDPCP
-
+ Nsp1
+ eIF1A
Quantity of cDNA, rfu
2 000
1 500
1 000
500
0
*
PreTC
TC

C

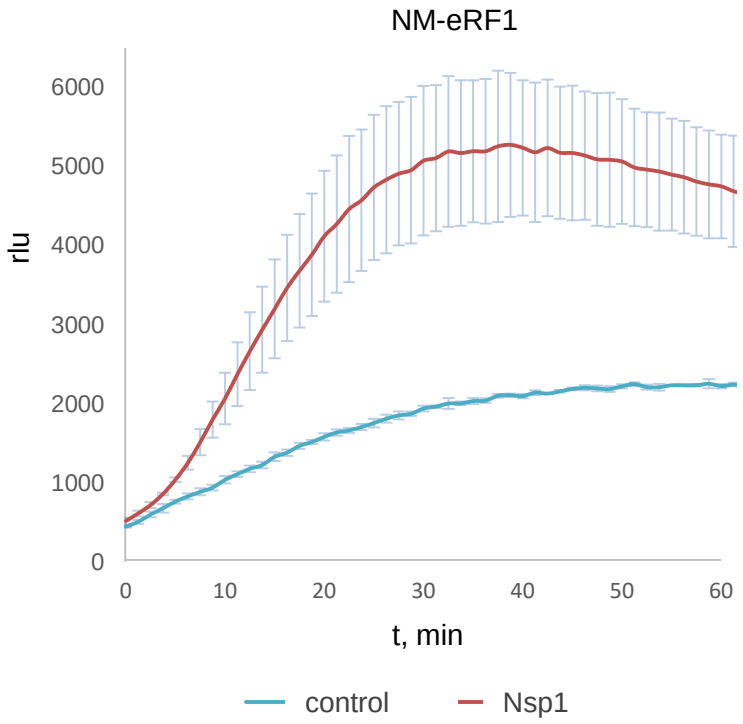
Peptide release assay
NM-eRF1
rlu
6000
5000
4000
3000
2000
1000
0
0
10
20
30
40
50
60
t, min
control
Nsp1

Fig 3

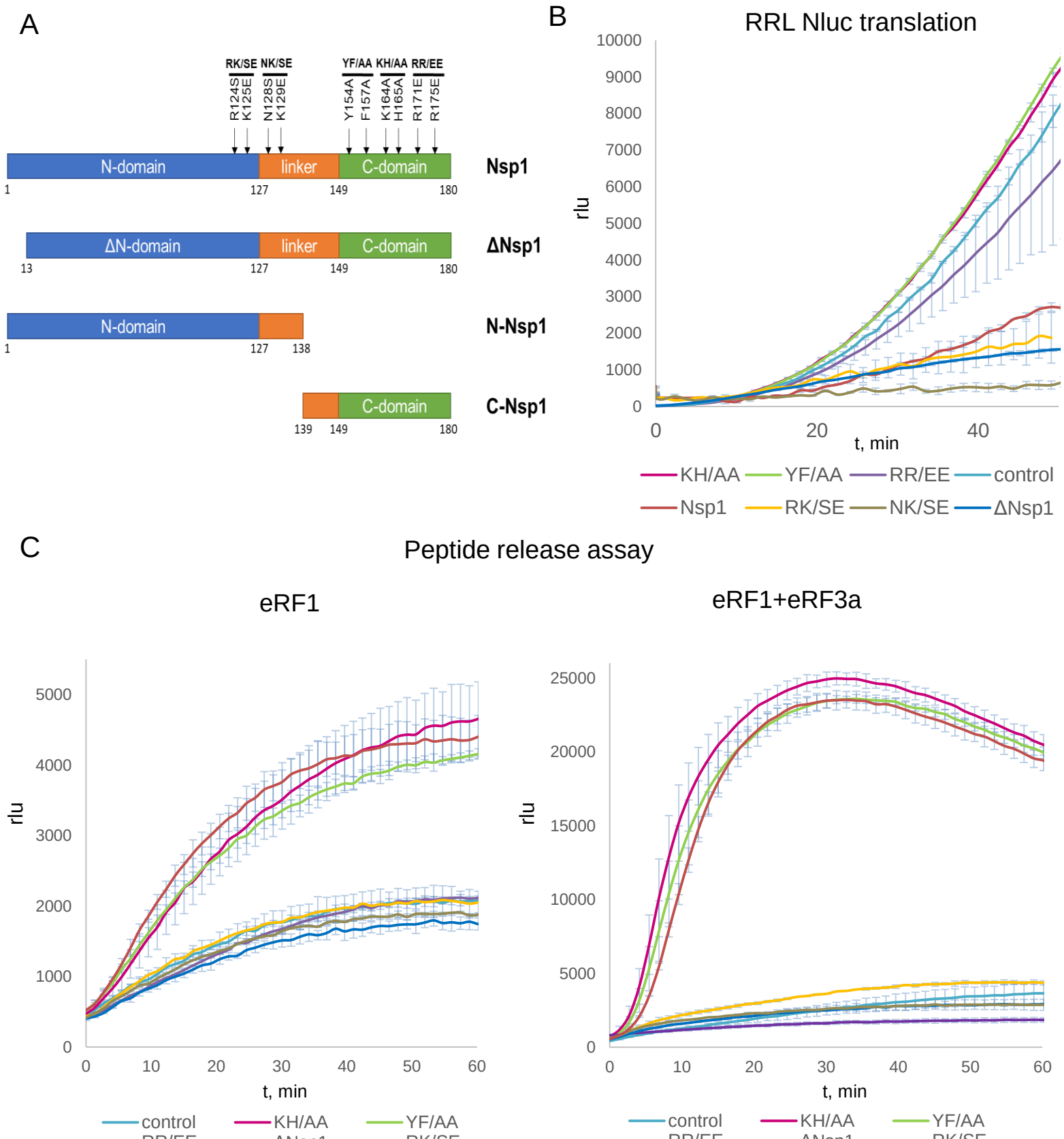
A
RK/SE NK/SE
R124S K125E N128S K129E
YF/AA KH/AA RR/EE
Y154A F157A K164A H165A R171E R175E
N-domain linker C-domain
Nsp1
1 127 149 180
ΔN-domain linker C-domain
ΔNsp1
13 127 149 180
N-domain
N-Nsp1
1 127 138
C-domain
C-Nsp1
139 149 180
B
RRL Nluc translation
rlu
t, min
KH/AA YF/AA RR/EE control
Nsp1 RK/SE NK/SE ΔNsp1
C
Peptide release assay
eRF1
eRF1+eRF3a
rlu
t, min
control KH/AA YF/AA
RR/EE ΔNsp1 RK/SE
NK/SE Nsp1

Fig 4

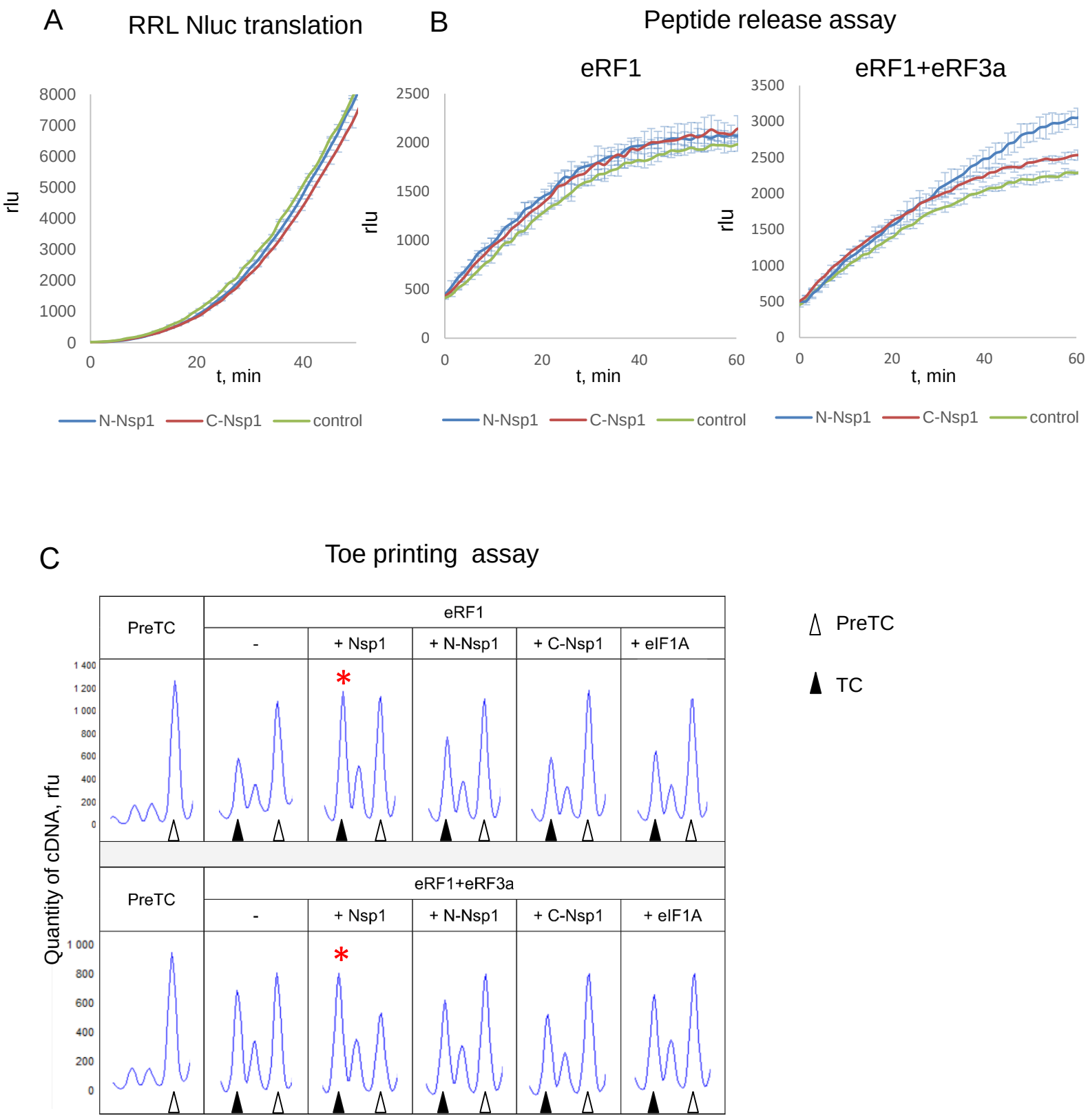
A
RRL Nluc translation
rlu
t, min
N-Nsp1
C-Nsp1
control
B
Peptide release assay
eRF1
eRF1+eRF3a
rlu
t, min
N-Nsp1
C-Nsp1
control
C
Toe printing assay
PreTC
eRF1
-
+ Nsp1
+ N-Nsp1
+ C-Nsp1
+ eIF1A
eRF1+eRF3a
Quantity of cDNA, rfu
PreTC
TC

Fig 5

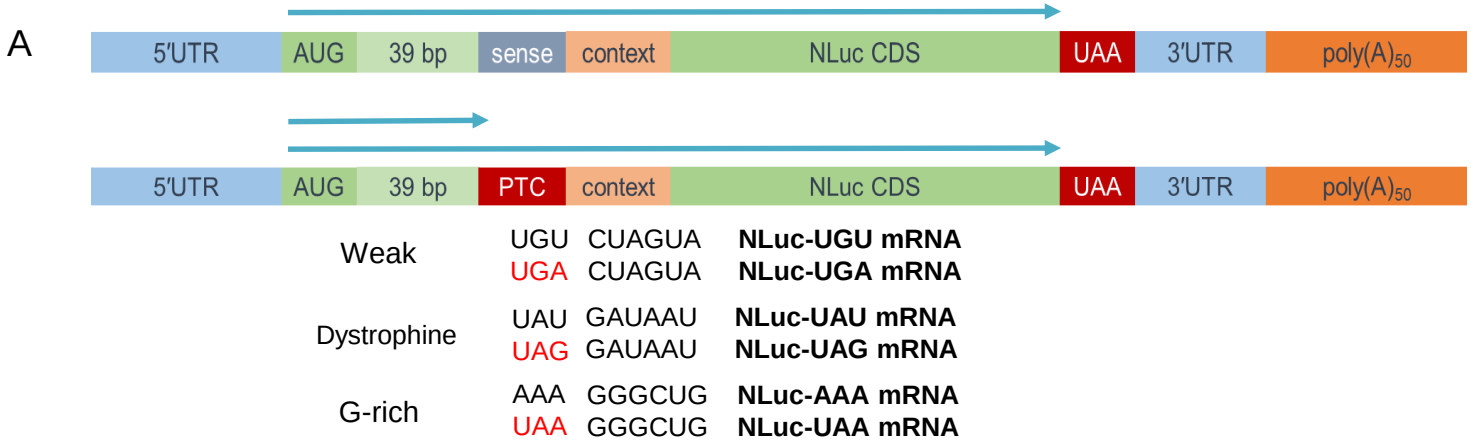
A
5′UTR
AUG
39 bp
sense
context
NLuc CDS
UAA
3′UTR
poly(A)50
5′UTR
AUG
39 bp
PTC
context
NLuc CDS
UAA
3′UTR
poly(A)50
Weak
UGU CUAGUA NLuc-UGU mRNA
UGA CUAGUA NLuc-UGA mRNA
Dystrophine
UAU GAUAAU NLuc-UAU mRNA
UAG GAUAAU NLuc-UAG mRNA
G-rich
AAA GGGCUG NLuc-AAA mRNA
UAA GGGCUG NLuc-UAA mRNA

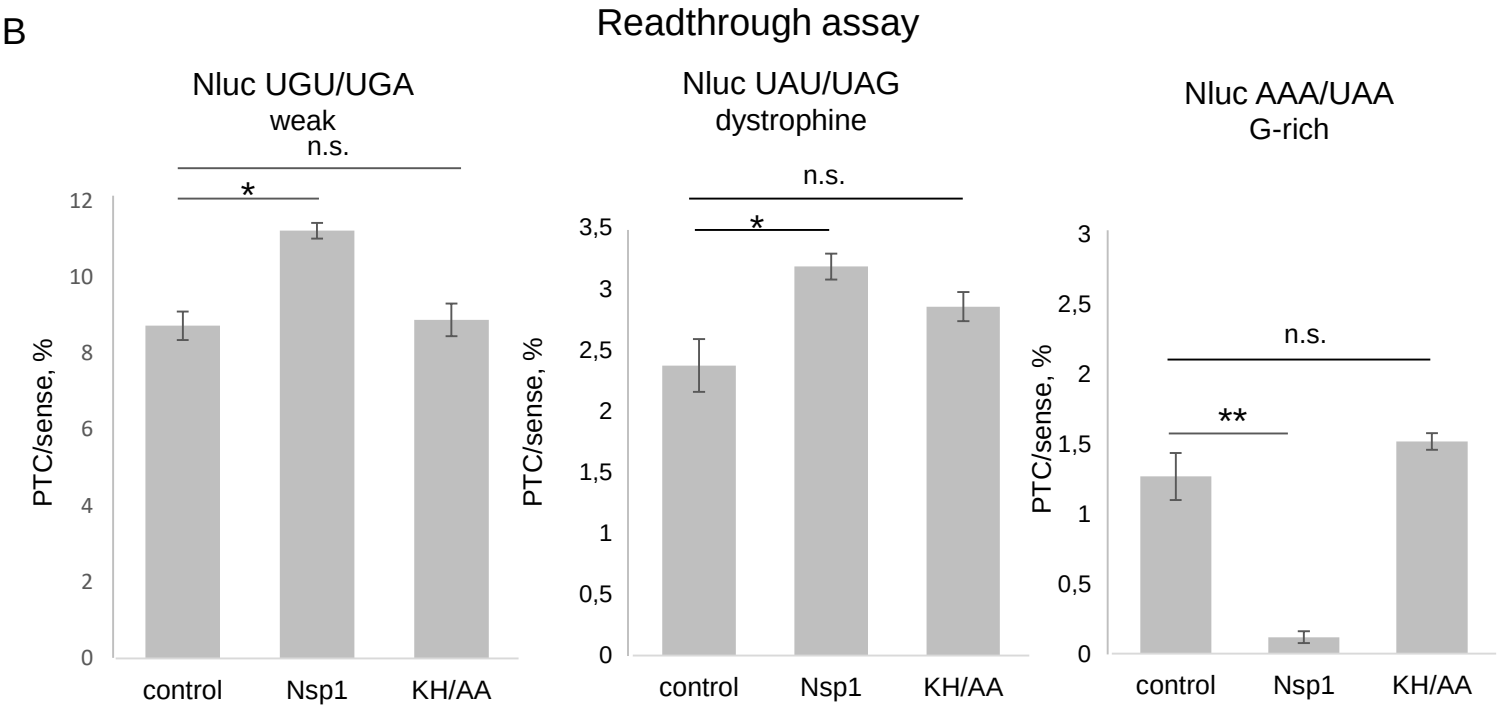
B
Readthrough assay
Nluc UGU/UGA
weak
n.s.
*
PTC/sense, %
control
Nsp1
KH/AA
Nluc UAU/UAG
dystrophine
n.s.
*
PTC/sense, %
control
Nsp1
KH/AA
Nluc AAA/UAA
G-rich
n.s.
**
PTC/sense, %
control
Nsp1
KH/AA

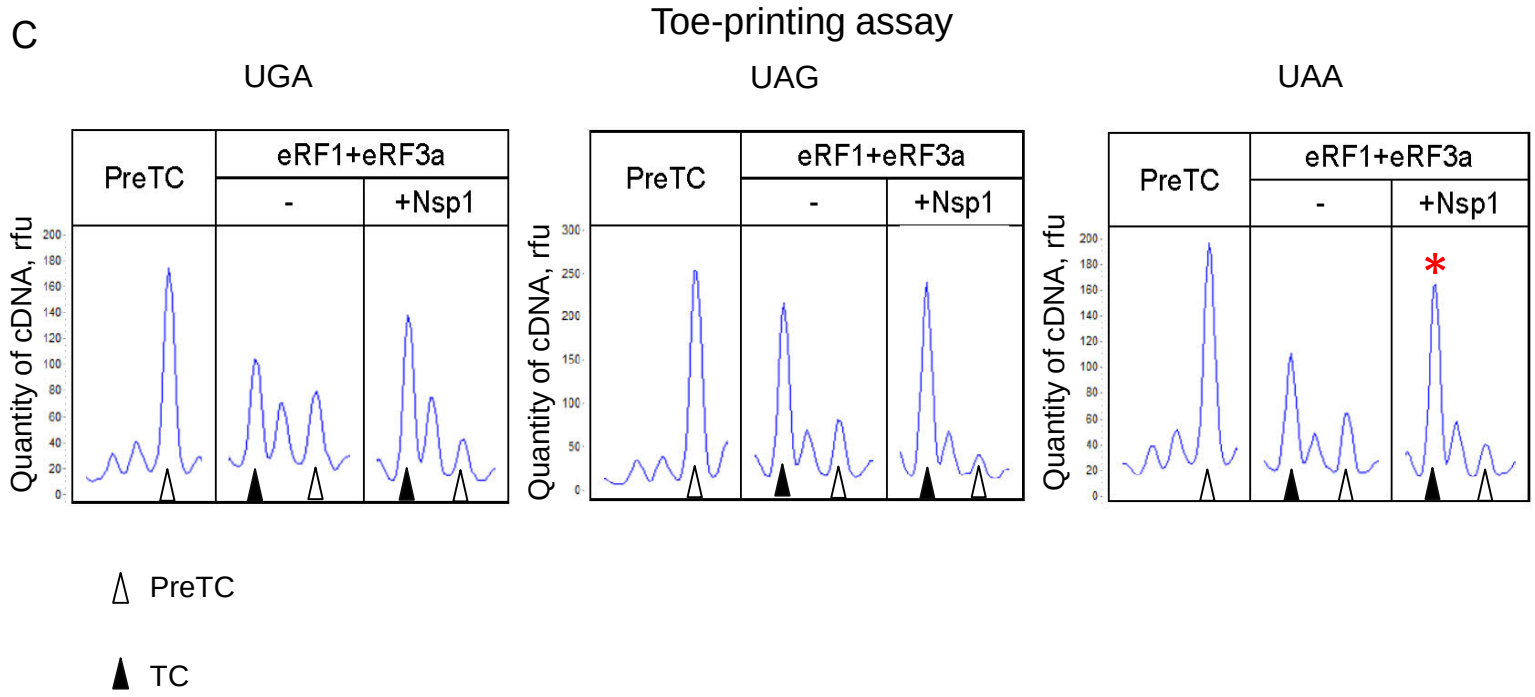
C
Toe-printing assay
UGA
UAG
UAA
PreTC
eRF1+eRF3a
-
+Nsp1
Quantity of cDNA, rfu
*
PreTC
TC

Fig 6

A

Peptide release assay

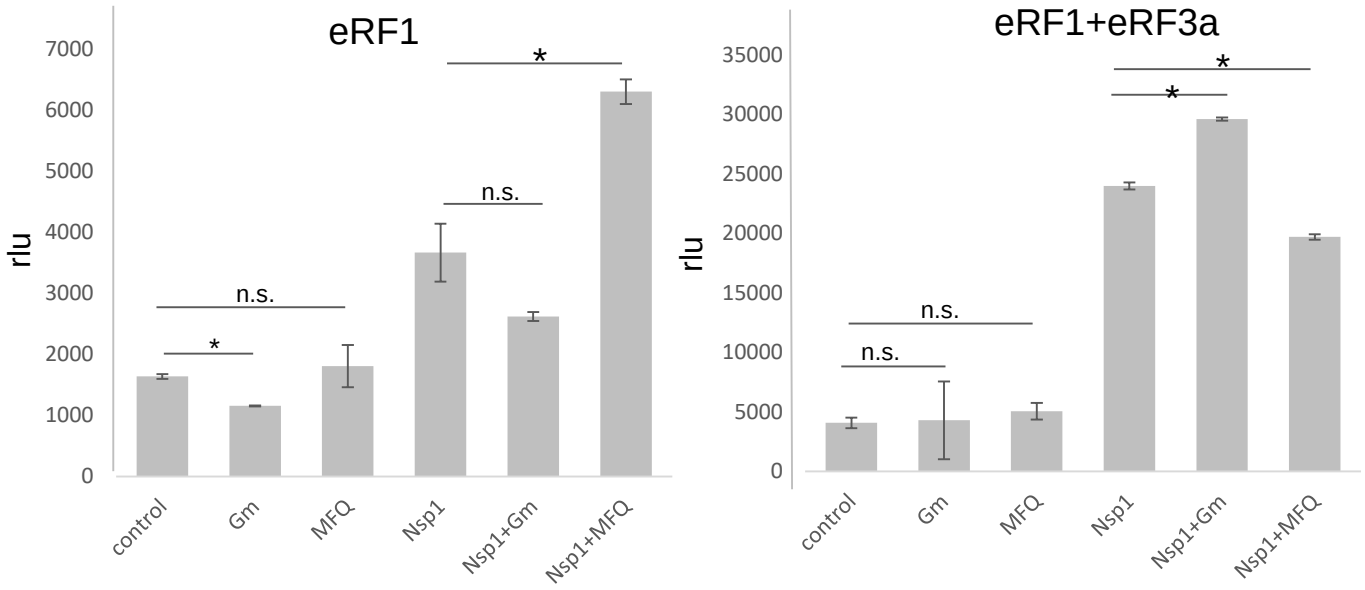

B

Toe printing assay

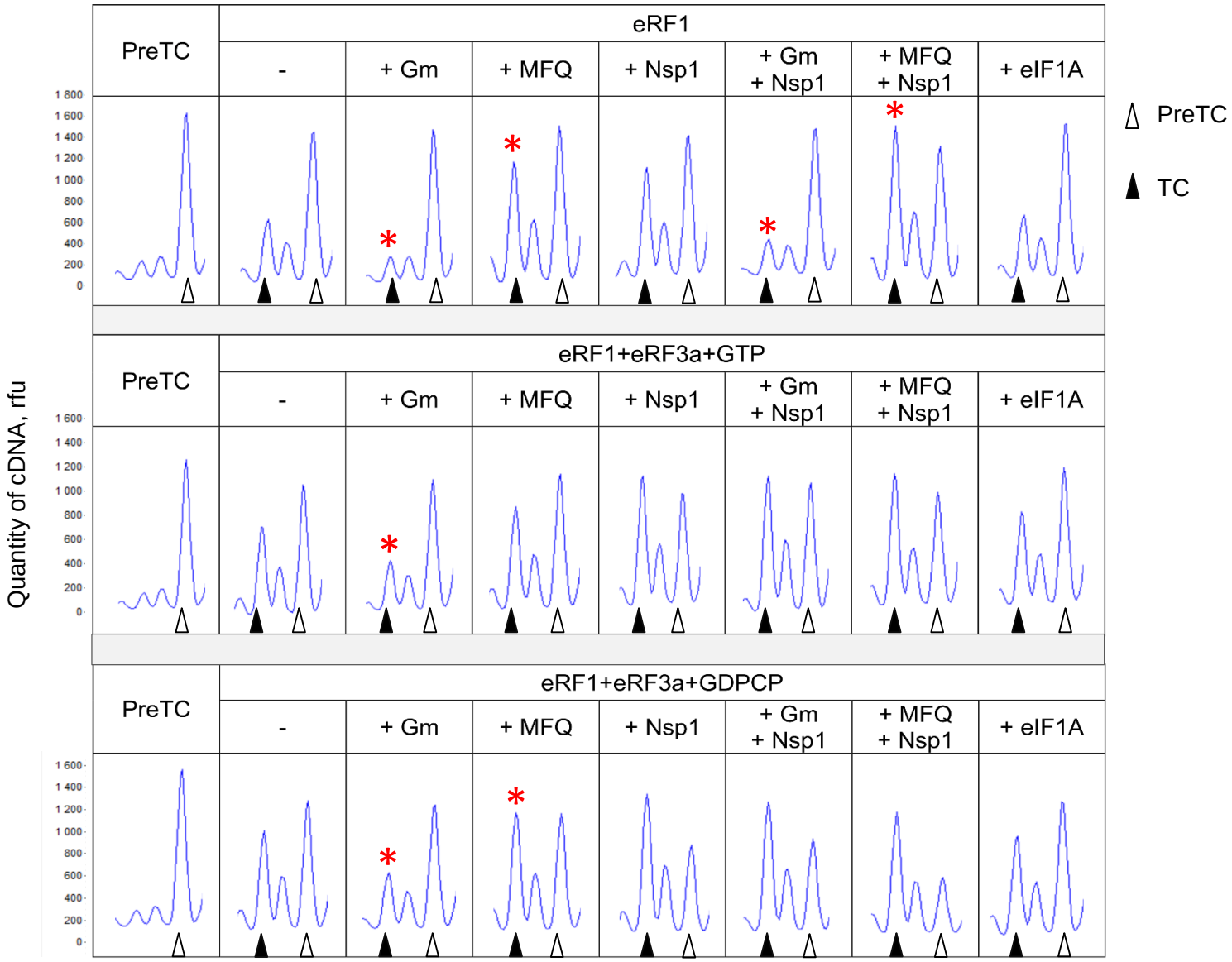

Fig 7

A

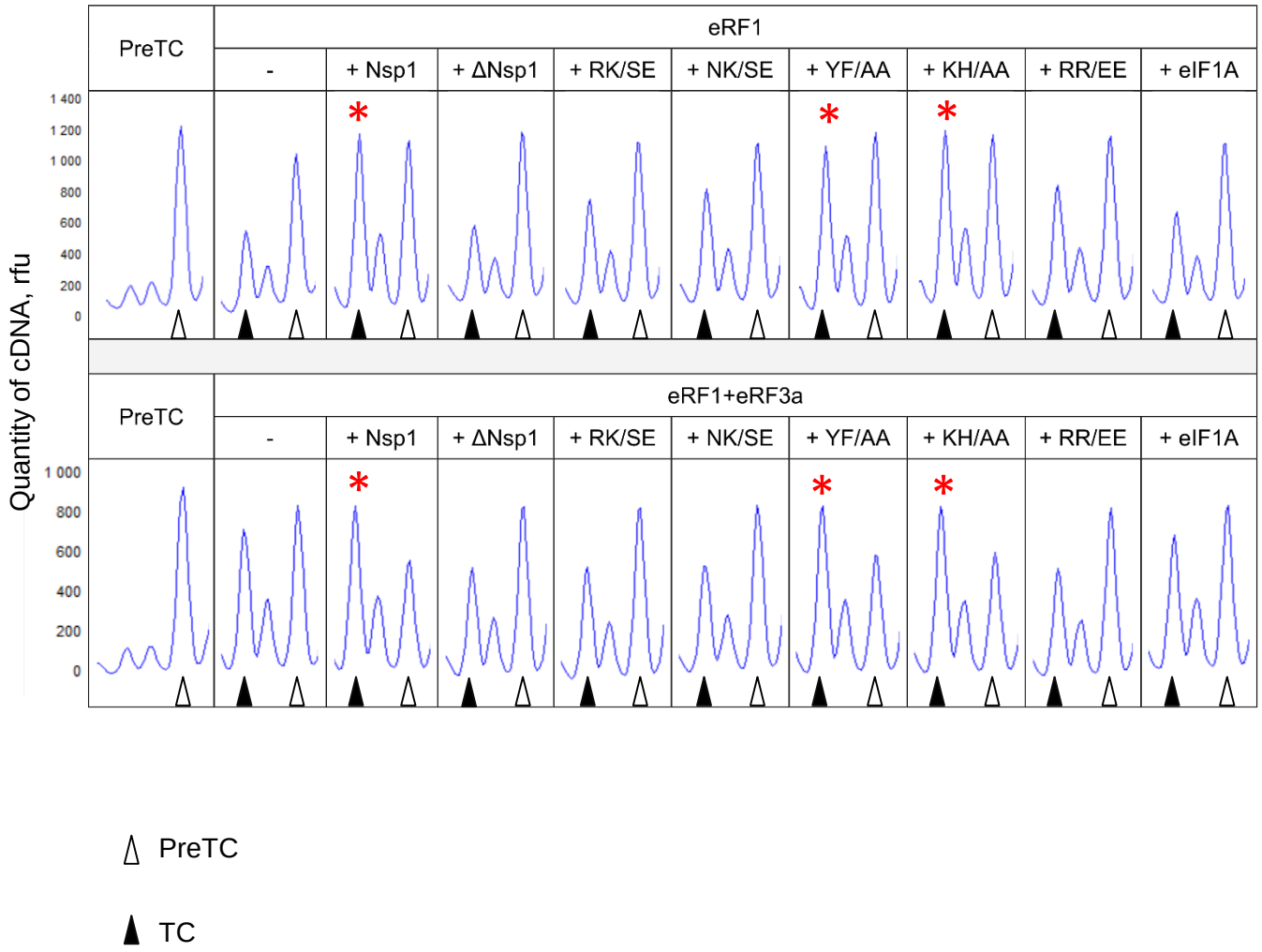
Toe printing assay
PreTC
eRF1
-
+ Nsp1
+ ΔNsp1
+ RK/SE
+ NK/SE
+ YF/AA
+ KH/AA
+ RR/EE
+ eIF1A
Quantity of cDNA, rfu
1 400
1 200
1 000
800
600
400
200
0
PreTC
eRF1+eRF3a
-
+ Nsp1
+ ΔNsp1
+ RK/SE
+ NK/SE
+ YF/AA
+ KH/AA
+ RR/EE
+ eIF1A
1 000
800
600
400
200
0
PreTC
TC

Fig S1

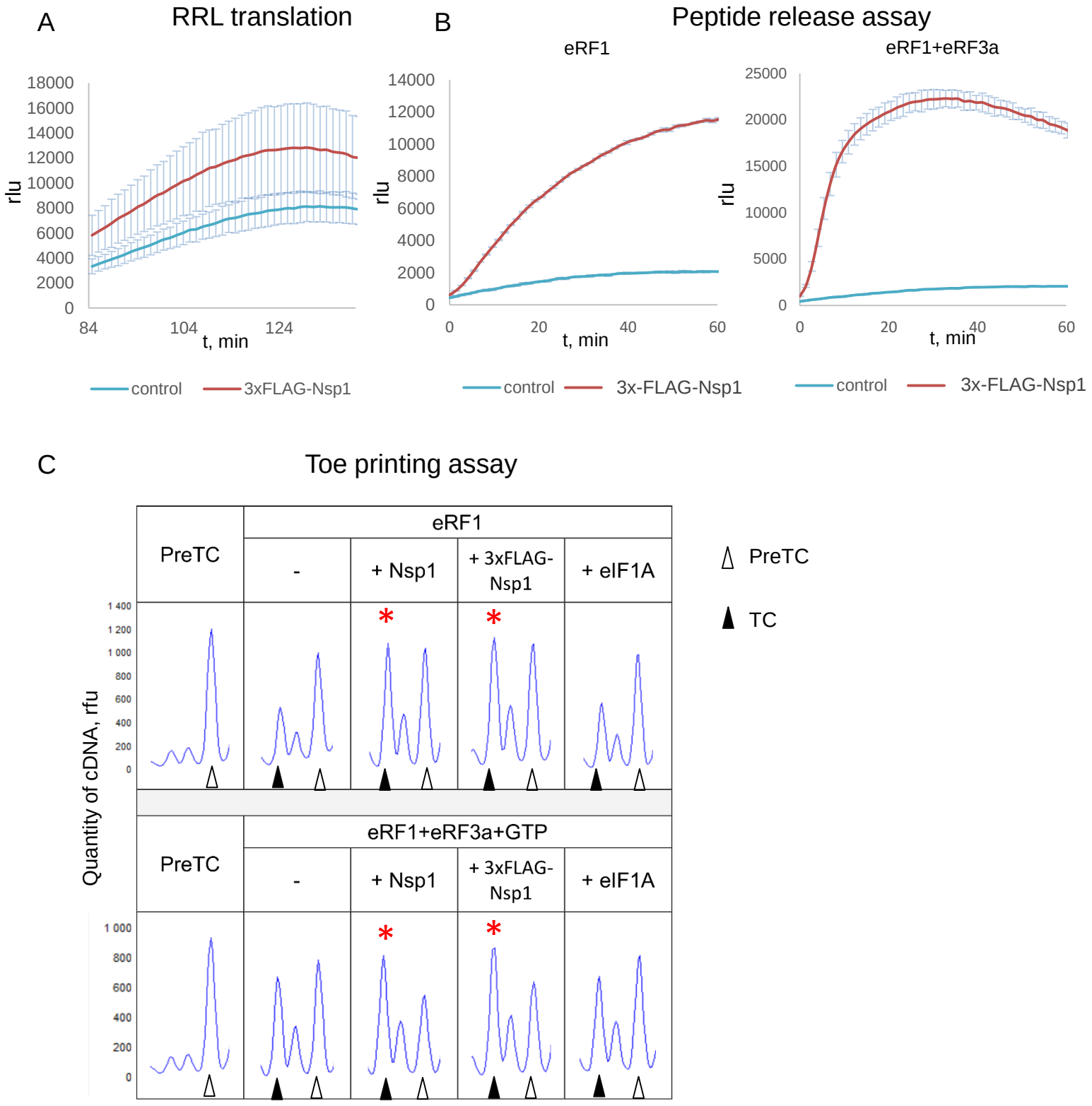
A
RRL translation
rlu
t, min
control
3xFLAG-Nsp1
B
Peptide release assay
eRF1
eRF1+eRF3a
rlu
t, min
control
3x-FLAG-Nsp1
C
Toe printing assay
PreTC
eRF1
-
+ Nsp1
+ 3xFLAG-Nsp1
+ eIF1A
eRF1+eRF3a+GTP
Quantity of cDNA, rfu
PreTC
TC

Fig S2